Bachelor Thesis

Digital implementation of motional feedback in a bass loudspeaker

by

Richard Eveleens & Leila Gottmer & Mart Haarman

to obtain the degree of Bachelor of Science
at the Delft University of Technology,
to be defended on Monday June 29, 2020.

Student numbers:	4665570, 4454448, 4586484	
Project duration:	April 20, 2020 – July 3, 2020	
Thesis committee:	Prof. dr. ir. W.A. Serdijn,	TU Delft, chairman
	dr. ir. G.J.M. Janssen,	TU Delft, supervisor
	dr. ir. A.J. van Genderen,	TU Delft

TU Delft

Abstract

This thesis report focuses on possible methods of digital implementation of motional feedback in a bass loudspeaker. In this thesis, the control system will be created for a monopole and a dipole speaker specifically. It does so by sketching the outlines of such a system and examining possible designs for the components required to suppress distortion which is mainly created by the speaker. This thesis shows that the digital implementation indeed allows filtering with very little latency but there are limitations in accuracy due to the conversion from the analogue to the digital domain. It is shown in this thesis that a partly analogue and partly digital system is desired for better error correction. A desired input-output gain of $30 = 29.54dB$ is achieved. The controller that is suggested is a controller based on the transfer function of the speaker. By transforming the input signal with the inverse of this open-loop transfer, the closed-loop transfer will be flattened. The instrumentation amplifier used to subtract the feedback signal from the input signal is designed such that the influence of the quantization noise is minimized. Loop-gain is added by the instrumentation amplifier, the controller and voltage-to-current amplifier. By creating loop-gain as much as possible using the digital implementation, noise is suppressed from $30dB$ up to $90dB$ within the range of frequencies of interest. The designed components in the motional feedback system allow a loop-gain up to $70dB$ and an input to output voltage gain of $30dB$ before instability occurs.

Preface

We would like to thank our supervisor Dr.ir. G.J.M Janssen for providing patient advice and guidance throughout this project. Moreover, we would like to thank all people involved with the planning of the Bachelor Graduation Project for adapting the rules due to the current pandemic, allowing for us to still complete the project this quarter.

This thesis project gave us new insights in the world of audio equipment and the community behind this world. It was a great pleasure to find out what kind of research and development has gone into products that we use in our daily lives and who the people behind these technologies are. We have found that this field of technology has a lot of potential to offer for us as electrical engineers in the making but also what we got to offer in the future.

Richard Eveleens & Leila Gottmer & Mart Haarman
Delft, June 2020

Nomenclature

Definitions

A_c	Common-mode gain.
A_d	Circuit gain
B	Magnetic flux density
$Bl(x)$	(non-linear) force factor on the voice coil.
e	Error signal
f	Feedback signal / frequency
$H(s)$	Transfer function of the total system
H	Magnetic field strength
i	Input signal
K_u	Ultimate gain
$K_{ms}(x)$	The product of non-linear displacement and stiffness.
$L_e(x,i)$	Magnetic flux based on displacement x and current i.
M	Voltage amplification between the adder and DSP
N_a	Noise added by the ADC, adder and voltage amplifier
N_k	Noise added by the current amplifier
N_m	Noise added by the accelerometer and speaker non-idealities
P_u	Ultimate period
S	Noise power given in $\frac{V^2}{Hz}$ or $\frac{V}{\sqrt{(Hz)}}$
S_a	Transfer function applied on N_a
S_k	Transfer function applied on N_k
S_m	Transfer function applied on N_m
V_{cm}	Common-mode (input) voltage
W_{cg}	Frequency at which a system oscillates with an uniform amplitude.
x	Displacement.

Abbreviations

ADC	Analog to Digital Converter
CMRR	Common-mode rejection ratio
DAC	Ditigal to Analog Converter
DMF	Digital Motional Feedback
DSP	Digital Signal Processing
EMF	Electromotive force
GM	Gain Margin
HD	Harmonic distortion
IMD	Intermodulation distortion
MFB	Motional feedback
PD	Proportional-Derivative
PID	Proportional-Integral-Derivative
PM	Phase Margin
Q factor	Quality factor
SNR	Signal to Noise Ratio
THD	Total Harmonic Distortion
VCCS	(Voltage controlled current source)

List of Figures

List of Tables

Contents

1 Introduction

Electro-mechanical transducers, such as loudspeakers, are non-ideal devices with several limitations. Loudspeakers generate distortions, for which a distinction can be made between non-linear and linear distortions. It should also be noted that loudspeakers behave differently at high and low signal amplitudes. This amplitude-dependent behaviour indicates that non-linearities are inherent to the system [13]. Moreover, additional spectral components are generated due to non-linearities in the system. These additional spectral components, however, are not present in the excited signal. The spectral components can be categorized as harmonic distortion (HD) and intermodulation distortion (IMD) [13]. Linear distortion is related to distortions of the intensity spread over the frequency spectrum [11].

Negative feedback can be implemented to suppress the unfavourable effects of the linear and non-linear behaviour of a loudspeaker. Negative feedback essentially reduces linear and non-linear distortion by feeding the output signal back to the input [5]. In addition, the operating bandwidth of the system is increased. Although negative feedback has plenty advantages, there still exist some disadvantages that have to be dealt with. Negative feedback can introduce instability. If the system becomes unstable the system will resonate at low and high frequencies [23]. Moreover, sensor noise is fed back as well [23]. These are two important effects to take into account when implementing feedback control.

In the early 1970s, a motional feedback system was designed by Philips [11] to suppress linear and nonlinear distortion in bass loudspeakers. Acceleration was measured using a piezoelectric accelerometer, which was mounted on the speaker cone. The recorded accelerometer signal was used in the feedback loop, in order to compensate for the distortion. It was found that the speaker performance was improved substantially.

Motional feedback concerning bass loudspeakers will be studied and applied in detail in this thesis. Two sub-groups exist, one of these subgroups will design the amplifier, the other subgroup will design the control system. This thesis will cover the design and implementation of the control system.

First, an in detail problem definition will be given which can be found in Chapter 2. Followed by, a programme of requirements, which is given in Chapter 3. Next, a bottom-up approach of the system followed by an in-depth description of the design process from start to finish will be discussed in Chapter 4 and 5, respectively. Finally, the designed implementation will be validated and discussed, followed by a conclusion.

2
Problem definition

In this section, an emphasis will be put on the various existing non-linearities. Furthermore, the current situation concerning motional feedback technology will be assessed in detail.

2.1. Non-linearities and distortion in a loudspeaker

It is assumed that loudspeakers behave linearly at small displacements. Besides, it can be assumed that loudspeakers behave non-linearly concerning the displacement at high amplitudes. This non-linear behaviour leads to signal components being generated that are nonexistent in the input signal. Figure 2.1 shows the output as a function of input for a linear and a non-linear amplitude response respectively.

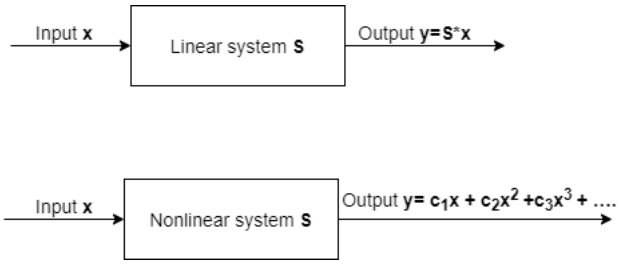

Figure 2.1: Block diagrams showing a linear and non-linear amplitude response, here x is the input, and y is the output. S represents a linear system in the upper block diagram and S represents a non-linear system in the lower block diagram.

Non-linearities can have detrimental effects on the system. For example, non-linearities can cause unstable behaviour, generate audible distortion and limit the acoustical output [13]. Most of these non-linearities are generally caused by the transducer principle, and they are therefore directly related to the geometry and material properties of the loudspeaker [13]. Three main loudspeaker cone position-dependent parameters can be considered essential when analyzing non-linearities in the system [18].

2.1.1. The force factor

The non-linear force factor $Bl(x)$ depends on the displacement x of the voice coil. $Bl(x)$ describes the coupling between the electrical and mechanical domain of an electromechanical transducer [13]. This non-linear coupling factor has no frequency dependency, thus it can be represented as a non-linear power series expansion. $Bl(x)$ has two main non-linear effects, namely;

- Any alteration of $Bl(x)$ will have an effect on the electro-dynamic driving force $F = i * Bl(x)$ considering $Bl(x)$ is a coupling factor [13].

- The second non-linear effect of $Bl(x)$ is the displacement dependency of the back EMF (electromotive force). This results in a variation of the electrical damping [13].

2.1.2. The stiffness

The suspension can be said to behave like a spring, and an almost linear relationship is present at small displacements. However, at large displacements, this is not the case[13]. The product of displacement and non-linear stiffness $K_{ms}(x)$ can be used to describe the restoring force $F = x * K_{ms}(x)$ [13]. From this, it can be concluded that the previously mentioned terms produce non-linear distortion in the time signal.

2.1.3. The inductance

It can be noted that the electrical input impedance is dependent on the position of the voice coil. Moreover, the current in the voice coil produces a magnetic field, therefore, the magnetic flux depends on the coil position as well as the magnitude of the current resulting in $L_e(x,i)$. Besides, the inductance is also dependent on the input current i, and this dependence is due to the non-linear relationship between the flux density B and the magnetic field strength H, $B = \mu(i)H$ [13].

2.1.4. Harmonic and intermodulation distortion

Harmonic and intermodulation distortion are usual measures of an audio system's non-linearity. The presence of harmonics and other spectral components, which are normally absent in the exciting stimulus, indicates that non-linearities are generated by the system [14].
The harmonic distortion associated with the output of the system can be determined by applying a sinusoidal function at the input. Higher-order terms c_k with $k \geqslant 2$ of the equation in Figure 2.1 will generate harmonic distortion. If the input is assumed to be a single tone signal of the form $x(t) = Asin(\omega_0 t)$ then the second-order term will yield a result given by Equation (2.1) [22]. From this, it can be seen that a DC level is created (at $\frac{c_2 A^2}{2}$), and a second harmonic distortion with amplitude $c_2 A^2/2$. Table 2.1 indicates which harmonics are generated for inputs up to order $k = 4$

$$c_2(Asin(\omega_0 t))^2 = \frac{c_2 A^2}{2}(1 - cos(2\omega_0 t)) \tag{2.1}$$

k	x^k	**harmonics**
1	$A[sin(\omega_0 t)]$	f_0
2	$\frac{A^2}{2}[1 + cos(2\omega_0 t)]$	DC, $2f_0$
3	$\frac{A^3}{4}[3sin(\omega_0 t) + sin(3\omega_0 t)]$	$f_0, 3f_0$
4	$\frac{A^4}{8}[3 + 4cos(2\omega_0 t) + cos(4\omega_0 t)]$	DC, $2f_0, 4f_0$

Table 2.1: Harmonics generated by the higher order terms, where A is the amplitude, and ω_0 is the radial frequency. The frequency of the harmonic is given by $f_0 = \omega_0/2\pi$, the DC component corresponds to $f_0 = 0$ Hz.

Table 2.1 clearly shows that spectral components are created at kf_0 with k taken from 1-4. This indicates that non-linearities will be present in the system.

The intermodulation distortion is obtained by using a two-tone input test signal [22]. Assuming that the two-tone input signal is of the from $x(t) = A_1 sin(\omega_1 t) + A_2 sin(\omega_2 t)$ the second-order output term will then be given by Equation (2.2) [22].

$$c_2(A_1 sin(\omega_1 t) + A_2 sin(\omega_2 t))^2 = c_2(A_1^2 sin^2(\omega_1 t) + 2A_1 A_2 sin(\omega_1 t) sin(\omega_2 t) + A_2^2 sin^2(\omega_2 t)) \tag{2.2}$$

From this equation, it can be seen that the first and last term on the right-hand side of the equation produces harmonic distortion. This harmonic distortion is located at frequencies $2f_1$ and $2f_2$. The cross-product term is responsible for the generation of IMD. It can be noted that IMD is only present when both input terms are present. The second-order IMD can be written in terms of cosines, this is given by Equation (2.3). From this it can be concluded that IMD generates sum and difference frequencies.

$$2c_2 A_1 A_2 sin(\omega_1 t) sin(\omega_2 t) = c_2 A_1 A_2[cos[(\omega_1 - \omega_2)t] - cos[(\omega_1 + \omega_2)t]]] \tag{2.3}$$

Table 2.2 displays the frequencies that are introduced for higher-order terms when a two-tone signal is taken as the input. Here k is taken from 1-4.

Research has shown that symmetrical non-linearity produces odd-order harmonics [13]. In addition, asymmetrical non-linearities produce even-order harmonics [13].

2.2. Situation assessment

Many solutions dealing with the above-stated distortion issues in a loudspeaker exist. One of these solutions is the implementation of a motional feedback (MFB) controller. The initial and current developments have to be investigated to make a proper situation assessment.

k	frequency components
1	f_1, f_2
2	$f_1 - f_2, f_1 + f_2$
3	$2f_1 + f_2, 2f_1 - f_2, 2f_2 + f_1, 2f_2 - f_1$
4	$f_1 + f_2\ , f_1 - f_2, 3f_1 + f_2, 3f_1 + f_2, 3f_2 + f_1, 3f_2 - f_1, 2f_1 + 2f_1, 2f_1 - 2f_2$

Table 2.2: IMD generated by the higher order terms, where A is the amplitude. The frequencies of the components are given by $f_1 = \omega_1/2\pi$ and $f_2 = \omega_2/2\pi$ respectively

2.2.1. Initial developments and implementation

In the early 1970s, Philips introduced MFB controlled loudspeakers [11]. The concept of MFB in loudspeakers involves cone movement measurements using a sensor, which is attached to the loudspeaker. This concept was applied together with a feedback loop to reduce the linear and non-linear distortion caused by loudspeakers. It was possible to obtain a flat amplitude response for low frequencies due to motional feedback, mainly because the acceleration of the cone could be made frequency-independent due to motional feedback [11]. One drawback of this feedback method was an increased noticeable resonance, meaning that a peak emerged in the amplitude response. This occurred because the feedback implementation caused a decrease of the resonance frequency. Besides this, the feedback implementation also caused the Q factor (quality-factor) to be increased [11]. Another advantage of this novel application was a significant reduction in loudspeaker size while retaining the low-frequency sound reproduction. What's more, systems with motional feedback were found to be rather expensive at the time.

2.2.2. Current implementation

This project is not the first to highlight motional feedback based on a digitally implemented controller. Grimm Audio has products (worth €40.000) on the market that claim to make use of DMF (Digital Motional Feedback) [21]. Even more, a Dutch company called PirateLogic is making products based on motional feedback audio. This company has low-frequency drivers with a so-called StarBass accelerometer built-in. PirateLogic has a speaker with an electronics set for motional feedback of which they claim the total set has specifications like a 1500 Hz DSP (digital signal processing) unit and $20dB$ motional feedback loop-gain.

The LS1s-DMF from Grimm Audio has white-papers that explain design choices for this product [21]. Similarities exist between their product and the one from this project. The feedback loop circuit has common components and a graphic from their last white-paper contains an image obtained from Sigma Studio. Sigma Studio is the software used to program the ADAU1777 DSP as well. The ADAU1777 is one of the DSP chips discussed in this thesis.
Both products make use of accelerometers as the main sensor for the motional feedback, which already implies that they are making use of a feedback loop in the system.

2.2.3. Future developments

The currently available solutions on the market that make use of MFB are rather expensive products of which the specifications can be largely improved. The example of PirateLogic's speaker shows that they have a $20dB$ loop-gain. In this thesis, it will be researched whether higher loop-gain is possible. It is in the scope of this project to add loop-gain and to suppress distortion, without destabilizing the system. The final goal should be achieving high-quality sound in bass regions without the use of expensive components, by making use of a feedback loop to reduce distortion. It is also desired to find out what types of noise can appear and in which parts of the system. Based on such a noise analysis, the system can be optimized to compensate not only for the distortion of the speaker itself but also for distortion added by other system components.

3
Programme of requirements

The requirements set for this project are a means to guide and limit the design process of the digital implementation of motional feedback in a bass loudspeaker. These requirements are based on the problem definition described in chapter 2. The requirements describe how the system, meaning the implementation of the motional feedback, should be designed and how the system should function. The requirements will be divided into mandatory requirements and trade-off requirements. The pre-assigned conditions for the project are formulated as well. These pre-assigned conditions may still be discussed and questioned during the thesis.

3.1. Requirement formulations

3.1. Mandatory requirements

- 3.1.1 The system must utilize motional feedback.
- 3.1.2 The voltage input to voltage output of the system should implement an average gain of 30 = 29.54dB in the frequency range of interest.
- 3.1.3 The minimum pass-band to be controlled for the monopole speaker control system is 20Hz to 250Hz.
- 3.1.4 The minimum pass-band to be controlled for the dipole speaker control system is 80Hz to 800Hz.
- 3.1.5 The maximum input to output phase shift in the frequency range of interest should be 45°.
- 3.1.6 The system should make use of a Digital Signal Processing (DSP) chip.

3.2. Trade-off requirements

- 3.2.1 Components added to the system should be designed to deliver minimized additional distortion.
- 3.2.2 The addition of loop-gain to the system should be optimized to the maximum achievable amount of loop-gain.
- 3.2.3 The costs of the product should preferably make the system a good alternative to high-end audio products.
- 3.2.4 Alternatives to the pre-arranged conditions should be discussed.
- 3.2.5 The system should suppress distortion.
- 3.2.6 The product should contribute to the environment by allowing smaller products to achieve the same (or better) quality as bigger audio products. (Less materials, less transport).
- 3.2.7 The Signal to Noise Ratio (SNR) inside the frequency range of interest should be at least 80dB.

3.2. Pre-arranged conditions

3.1. The provided audio signal for the monopole has a frequency range from 20Hz to 80Hz.

3.2. The provided audio signal for the dipole has a frequency range from 80Hz to 300Hz.

3.3. The DSP chip of interest is the ADAU1777 [4].

3.4. The feedback control for the feedback loop is based on data from an accelerometer.

3.5. Measurements used for this project are based on a VCCS (voltage controlled current source) amplifier system.

4

Bottom up approach

Tackling the problems described in Chapter 2 is done using the motional feedback concept. In this chapter, the general design of the control system [10] surrounding this motional feedback concept will be covered starting from the speaker up to the final system. For every component added to the system, its purpose and influence on the system will be discussed briefly. Therefore, this chapter will function as a technical introduction to the system before the design and implementation will be elaborately explained in Chapter 5.

4.1. The speaker (the plant)

The speaker (the plant in the control system) is the component that should be controlled to obtain a flat frequency response across the frequency band of interest. The frequency response of the speaker as an individual component is not at all flat, and this will be compensated for using the control system. The system containing only the speaker can be modelled as is shown in Figure 4.1, resulting in the transfer function given in Equation (4.1).

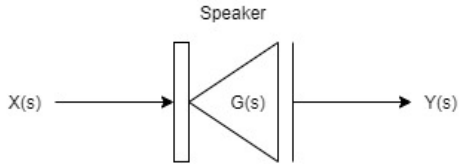

Figure 4.1: System schematic solely containing the mono-pole speaker (the plant).

$$\frac{Y(s)}{X(s)} = H(s) = G(s) \tag{4.1}$$

4.2. Accelerometer and negative feedback loop

Controlling the system will be done using a negative feedback loop. To be able to construct this negative feedback loop, the output should be obtained in some way and fed back to the input of the system. The "recording" of the output signal will be done using an accelerometer. This accelerometer will convert the acceleration of the speaker to a voltage, which can be used in the feedback system. The assumption is made that the acceleration to voltage conversion of the accelerometer will be constant and equal to 1 in the frequency range of interest. By making this assumption, the accelerometer response can be left out of the transfer function. Another reason why this assumption is made is that only a theoretical analysis of the system will be performed during this project. If a physical model would be made, these assumptions will most likely not hold. The gain in the feedback loop (discussed later) should be adjusted to accommodate for this unknown conversion rate. The schematic after implementing the negative feedback loop and the corresponding transfer function can be found in Figure 4.2 and Equation (4.2). Signals f, i and e can be found in the figure, they represent the feedback signal, input signal and error signal, respectively. Subtracting f from i will be done in an analogue way using an adder due to reasons which will be covered later on.

$$H(s) = \frac{G(s)}{1 + A(s) * G(s)} = \frac{G(s)}{1 + G(s)} \tag{4.2}$$

4.3. Voltage to current amplifier

Speakers can be driven using current or voltage sources and choosing one of the two has a great impact on the performance of the speaker. Speakers react better when they are driven by a current source and this is why

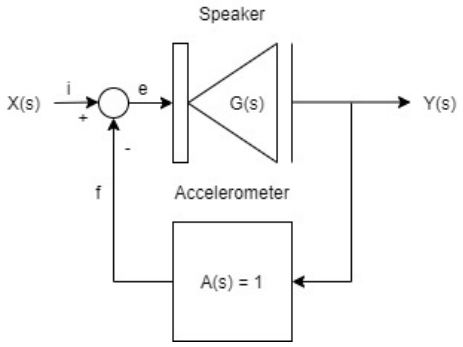

Figure 4.2: System schematic containing the speaker and the negative feedback loop implemented using the accelerometer.

a voltage to current amplifier is used to drive the speaker. Besides this, the cone oscillation is proportional to the current and thus the measured response by the accelerometer matches better with a current-driven speaker. The specifics regarding this amplifier are covered by the other subgroup in this project [1]. In the design process of the control system, several characteristics of the amplifier, obtained from the other subgroup, will be used. The most important assumption regarding this amplifier is that its response is flat inside the frequency range of interest and thus adds a constant loop-gain to the system. The schematic after inserting the voltage to current amplifier can be found in Figure 4.3, with the corresponding transfer function given in Equation (4.3).

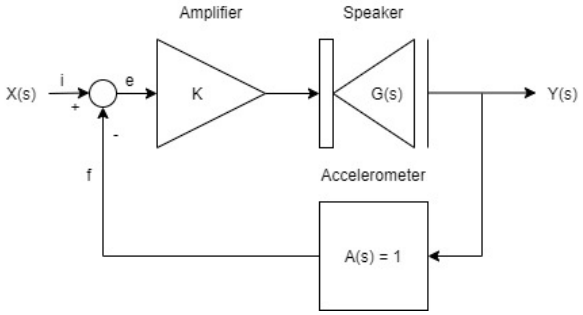

Figure 4.3: System schematic containing the speaker, the negative feedback loop and the voltage to current amplifier.

$$H(s) = \frac{K * G(s)}{1 + K * G(s)} \tag{4.3}$$

4.4. System gain

Besides a flat response in the frequency band of interest, the system should also implement a gain from the input to the output. Even though this will have a negative influence on the loop-gain, it is one of the system requirements to amplify the input signal such that the volume produced by the speaker is sufficiently amplified. The gain can be implemented by adding a gain in the feedback loop. The schematic representing this and the corresponding transfer function can be found in Figure 4.4 and Equation (4.4). By analysing the transfer function, the influence of component P on the input to output gain can be analysed. When making the assumption that the loop-gain is sufficiently large, the derivation shown in Equation (4.5) can be made. This shows that the input to output gain is the inverse of the gain in P. To be able to have an input to output gain, P should thus attenuate the feedback signal.

$$H(s) = \frac{K * G(s)}{1 + P * K * G(s)} \tag{4.4}$$

$$H(s) = \frac{K * G(s)}{1 + P * K * G(s)} \approx \frac{K * G(s)}{P * K * G(s)} = \frac{1}{P} \tag{4.5}$$

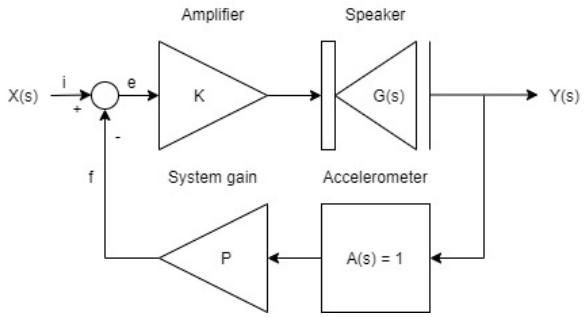

Figure 4.4: System schematic containing the speaker, the negative feedback loop, the amplifier and the system gain making it possible to have a gain from in to output.

4.5. Controller

To obtain the desired flat frequency response in the frequency range of interest, a digital controller will be implemented in the system. The digital controller makes it possible to precisely influence the response at specific frequencies. Besides adding a specific gain at certain frequencies, the digital controller will also filter out frequency components which should not be controlled. The digital component used to do this signal processing will be the ADAU 1777 chip [4], which is specifically designed to perform signal processing with very low latency. Since the signals will be processed digitally, an Analog to Digital Converter (ADC) and a Digital to Analog Converter (DAC) are required to perform the necessary signal conversion. The controller and the converters are added to the system schematic as shown in Figure 4.5 and the transfer function is given by Equation (4.6).

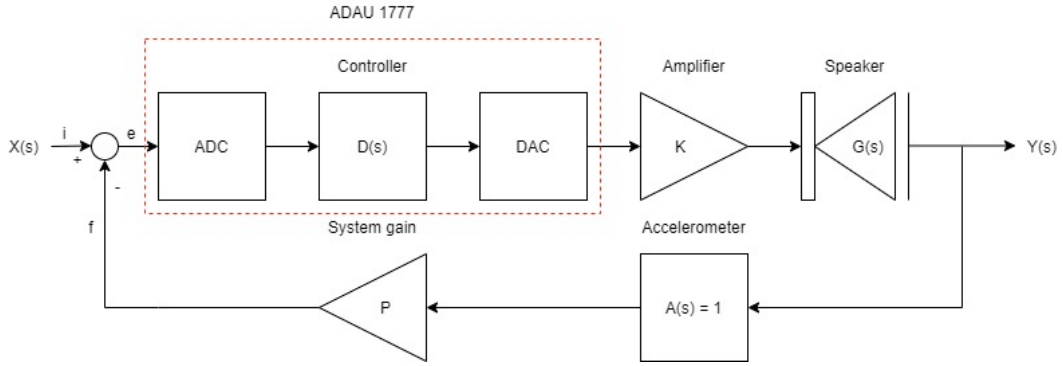

Figure 4.5: System schematic containing the speaker, the negative feedback loop, the amplifier, the system gain and the controller which will implement filtering and precise signal processing to increase performance and stability of the system.

$$H(s) = \frac{D(s) * K * G(s)}{1 + D(s) * P * K * G(s)} \tag{4.6}$$

4.6. Voltage amplifier

To be able to add loop-gain until instability occurs, an analogue amplifier will be used. The main reason for this is that that the error signal (e) can be very small in terms of voltage, voltages with the size of $10nV$ can still appear. When such small voltages occur, the quantization noise originating from the ADC of the ADAU can be larger than the error signal e, thus making error signals in this order of magnitude pointless. When an analogue amplifier is put in front of the ADC, the error signal will be amplified and the quantization noise of the ADC will thus have relatively less influence on the quality of the digital representation of the provided analogue signal e. This is the main reason why it was decided to add loop-gain in an analogue manner instead of digitally. Adding this component to the system results in the system schematic given in Figure 4.6 and the transfer function given in Equation (4.7).

$$H(s) = \frac{M * D(s) * K * G(s)}{1 + M * D(s) * P * K * G(s)} \tag{4.7}$$

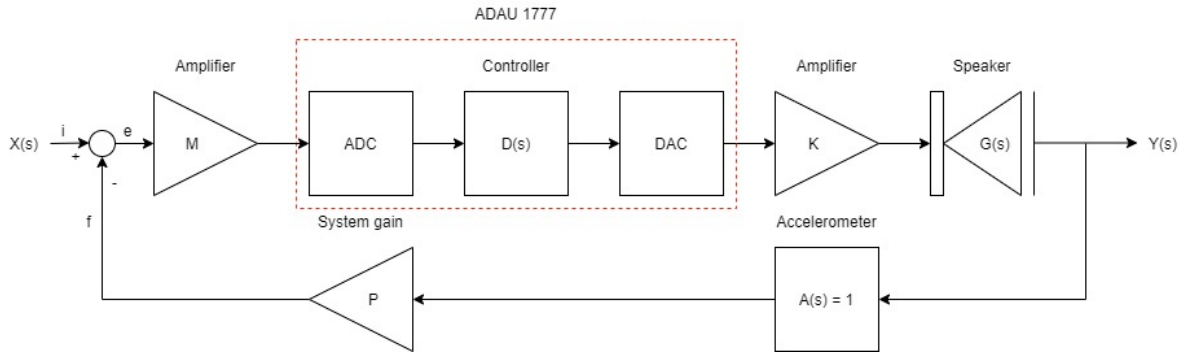

Figure 4.6: System schematic containing the speaker, the negative feedback loop, the amplifier, the system gain, the controller and the analogue amplifier which adds loop-gain to the system.

4.7. Noise sources

Thus far, it was assumed that the components in the system behave ideally. This is of course not the case and thus several noise sources will be added to the system. For these noise sources, models will be made to analyse what their influence on the system will be. Three major noise sources will be modelled:

- N_A represents the quantization noise coming from the ADC of the ADAU chip. The source will be located just before the ADC since this is where the noise will be added to the system. Other noise sources originating from the ADAU are considered negligible compared to the quantization noise.
- N_K represents the noise coming from the voltage to current amplifier. The characteristics of this noise are given by the amplifier subgroup.
- N_M represents the noise generated by the accelerometer. A model for this noise will be made by analysing measurements done using the speaker with the accelerometer attached to it.
- N_L represents the distortions from the loudspeaker which is modelled as noise.

Noise coming from other components is considered negligible in comparison to these three noise sources. Implementing these sources results in the system schematic given in Figure 4.7. The functions representing the propagation of N_A, N_K, N_M and N_L are given in Equations (4.8), (4.9), (4.10) and (4.11) respectively. The transfer function for N_a (S_a), will decrease when the voltage amplification M increases. This means that adding the major amount of loop-gain in the very beginning of the system will decrease the quantization noise. The transfer function S_k, corresponding to N_k, shows that an increase in loop-gain will decrease the influence of noise source N_k on the system. It is thus expected that this noise will be greatly suppressed by the control system. The transfer function S_m, corresponding to N_m, shows that the noise originating from the accelerometer can only be suppressed by decreasing the loop-gain. Since this is not desirable for the system performance, it is possible to conclude that this noise source will not be suppressed. But the transfer function of the total system $H(s)$ will give an input to output gain, one can still say that N_m will be suppressed since it will not receive the gain that the input signal will receive. The transfer function S_L of N_L shows that the distortions provided by the speaker will be suppressed when loop-gain is added to the system. The components that can add loop-gain to suppress these distortions are M, $D(s)$, K and $G(s)$. The derivations of all the transfer functions are given in Appendix A.

$$S_A(s) = \frac{D(s) * K * G(s)}{1 + M * D(s) * P * K * G(s)} \tag{4.8}$$

$$S_K(s) = \frac{G(s)}{1 + M * D(s) * P * K * G(s)} \tag{4.9}$$

$$S_M(s) = \frac{M * D(s) * P * K * G(s)}{1 + M * D(s) * P * K * G(s)} \tag{4.10}$$

$$S_L(s) = \frac{1}{1 + M * D(s) * P * K * G(s)} \tag{4.11}$$

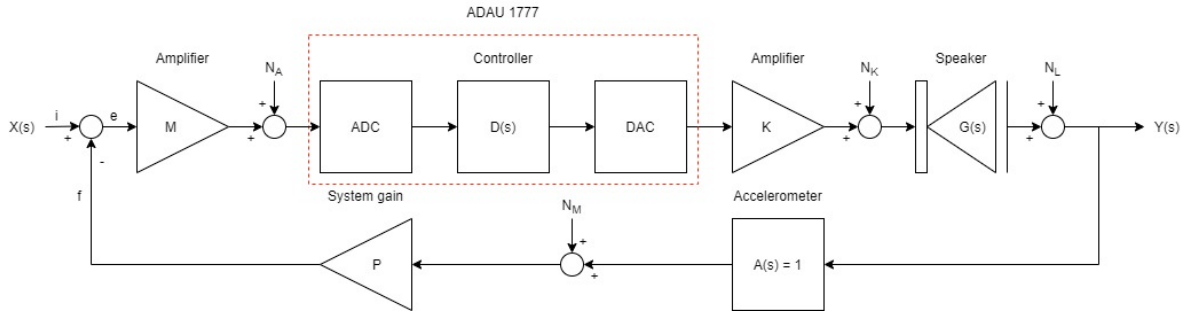

Figure 4.7: System schematic containing the speaker, the negative feedback loop, the amplifier, the system gain, the controller, the analogue amplifier and the noise sources.

5
Design process

In this chapter, the components of the control system will be described in more detail. In contrast to the general description given in chapter 4, the speakers for which this system was specifically designed will be used to show how the components influence the system performance. Besides the elaborate description of the system components, the system as a whole will be analysed and the influence of noise and non-linearities will be shown. The mono-pole speaker will be used to describe the influence of the components and similar results for the dipole can be found in the appendix. The control system of the mono-pole speaker should provide a flat frequency response with a voltage to voltage gain of 30 in at least the frequency range $20Hz$ to $250Hz$. For the dipole filter, again a voltage to voltage gain of 30 is required but in at least the frequency range $80Hz$ to $800Hz$.

5.1. Speaker

The plant is the component which will be controlled using the control system. For this project this is the speaker. As stated before, the speaker should be controlled in such a way that the frequency response is flat in the requested pass-band. As an individual component, the frequency response and phase response of the mono-pole speaker looks like the response given in Figure 5.1. This response is measured using a setup consisting of a current amplifier connected to the loudspeaker connected to the accelerometer. The response using a voltage source at the input could also be used. Since the speaker in the actual system will be driven by a current source, the speaker response coming from a current driven speaker is chosen. The red dotted lines indicate the minimum pass-band which should be controlled. A similar plot for the dipole speaker can be found in Figure C.1. The model of the non-linearities coming from the speaker will not be derived in the upcoming subsections but will be combined with the noise analyses of the accelerometer in Section 5.2.1. A problem with the frequency responses as given in the figures is that it is unsure how the y-axis is defined. In other words, it is unclear what voltage represents the 0 dB point. For now it is thus assumed that the speaker consists of the speaker itself and an unknown amount of gain. The fact that this gain is unknown should not be a major problem since it only influences the loop-gain of the system. If a real life adaptation would be made, the loop-gain of other components should be altered to accommodate for this.

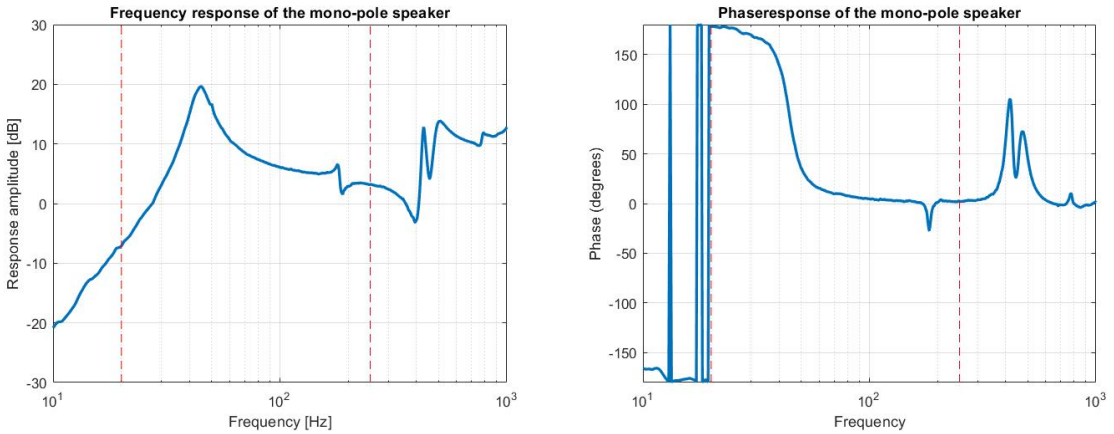

(a) The frequency response of the speaker.

(b) The phase response of the speaker.

Figure 5.1: Frequency and phase response of the mono-pole speaker. The red lines indicate the minimum pass-band which should be controlled and receive the specified gain.

5.1.1. delay

The speaker does not only have an irregular frequency response and non-linear behaviour but also induces some delay on the system. Since delay in the system can cause the system to become unstable, the delay should be found to check whether it is destructive to the system or not. The delay of the speaker is found by analysing the impulse response of the system. The small time instance at the beginning of the impulse response of the speaker is an indication of the delay of the speaker. The beginning of the impulse response for the mono-pole speaker can be found in Figure 5.2 and a similar plot for the dipole speaker can be found in Figure C.2. In these figures, the red lines indicate the time instance that is considered the delay time. Since there are very little samples present at these small time instances, a very robust delay determination is not possible. The approximation of the delay inflicted by the mono-pole speaker is $210\mu s$ and for the dipole speaker, this is $160\mu s$.

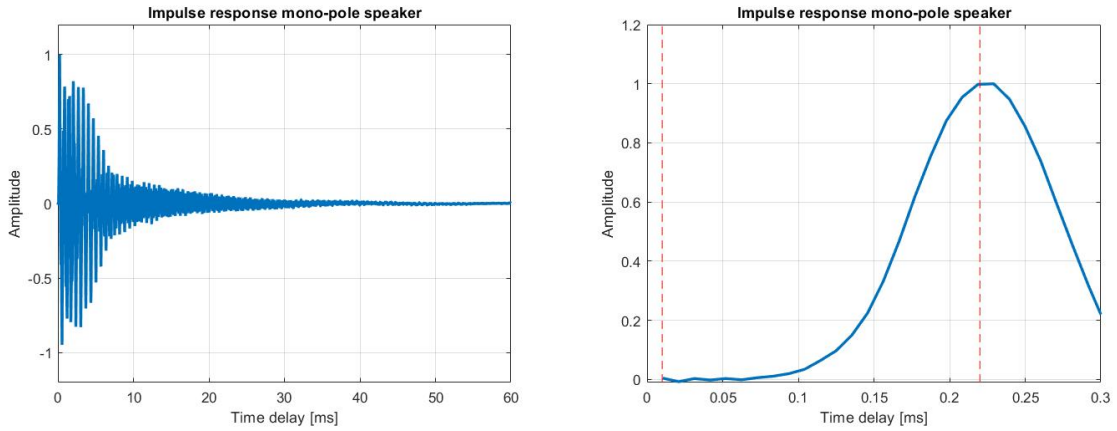

(a) Impulse response of the speaker.

(b) Zoomed in impulse response to determine the delay of the system.

Figure 5.2: Impulse response of the mono-pole speaker used to determine the delay it inflicts on the system. The red lines indicate the time instance which is considered to represent the delay of the speaker.

5.1.2. Modelling the speaker

To be able to check the stability of the system it is desirable to model the speaker and thus find the poles and zeros of the estimated transfer function of the speaker. This model will also be used later on in the design of the controller. Modelling the transfer function was done using the transfer function estimation function in MATLAB. This function models a transfer function given an input and output to the system in question. As was discussed in the practicum of the Telecommunications A course, the input signal should have an auto-correlation which has a major peak at the 0^{th} sample to make sure that the results will be optimal [2]. A good example of a signal with such an auto-correlation is a random signal and this was thus used during the modelling of the system. The frequency range chosen for the estimation of the transfer function of the mono-pole speaker is $10Hz$ to $1kHz$. Limiting the range over which the model is made results in less poles being necessary to make a good estimation and thus decreases the complexity of the model and increases the accuracy of the model. Frequencies outside of the specified band are also not of interest since filters will be used to make sure these frequencies will not be controlled and thus do not disturb the system. For the monopole speaker, the estimation of the frequency response and the corresponding phase response is given in Figure 5.3. This is a 15^{th} order system. In the figures, the range between the green dotted line indicates the frequency range for which the model was designed. Similar results for the dipole filter can be found in Figure C.3 which is made using a 25^{th} order system modelled in the frequency range $20Hz$ to $2kHz$.

5.1.3. conclusion

Both speakers do not represent at all a flat frequency response for the frequency range of interest, this will be accommodated for with a negative feedback control system. For both speakers, a model is created which approximates the frequency and phase response in a certain frequency range. The delay coming from the speakers is $210\mu s$ and $160\mu s$, for the monopole and dipole speaker, respectively. Non-linearities caused by the speakers are not taken into account during modelling but a model of this will be presented in Section 5.2.1. The major problem with the current frequency response is that the scaling of the axis is unknown and it

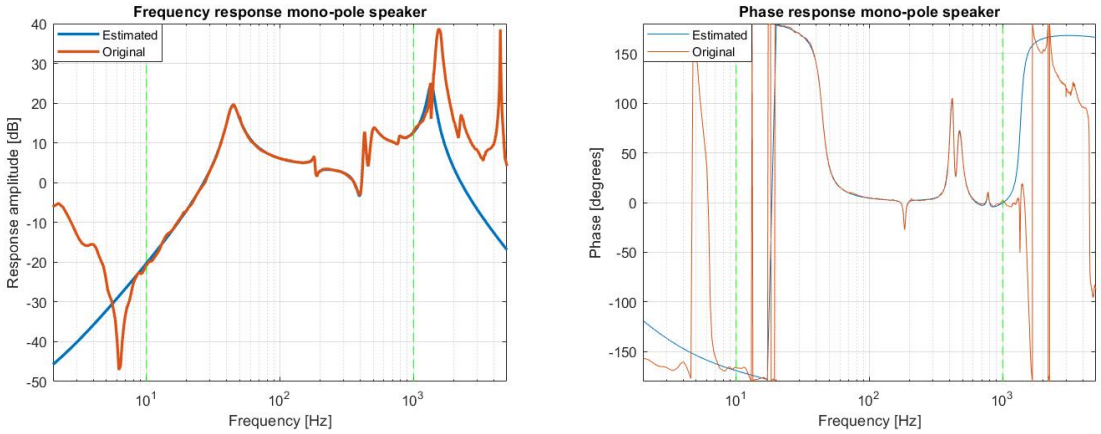

(a) The actual and the model of the mono-pole frequency response.

(b) The actual and the model of the mono-pole phase response.

Figure 5.3: Modelling the mono-pole speaker into a transfer function. The frequency range indicated by the green dotted lines indicate the range for which the speaker was modelled.

is thus unknown what the decibel scale actually represents in terms of voltage. For now, this is assumed to be a constant unknown gain which adds to the loop-gain and it is thus not required to do more major research on this. If a physical system would be created, this constant gain could be translated back to the loop-gain implemented in M.

5.2. Negative feedback loop

The speaker has distortion and the desired outcome of this project is to suppress this distortion. The plant is represented by the loudspeaker and this plant has to be controlled. One way this can be done is by means of a negative feedback loop, which is the main scope of this project. The feedback loop in this system contains multiple components and these will be discussed here from the sensor up to the controller.

5.2.1. Accelerometer

The first step in controlling is knowing what to control, more specifically, knowing what the output for the system is. For this project, measuring the output is done using an accelerometer. Although it is said to use an accelerometer for this thesis, some alternatives can still be considered. An accelerometer has to be attached to the speaker's cone, which adds mass and changes the speaker characteristics. The accelerometer may be lightweight but so is the cone, hence, added mass will be noticeable. Besides, every component added to the system won't be an ideal component. The same goes for the accelerometer, it introduces noise and a response that is also shown in this section.

The current accelerometer

In the research and simulations, the data that has been used was obtained from measurements using an accelerometer. It was however always assumed that the measurements of the accelerometer would have a $0dB$ gain but rather it has an unknown gain response. It seemed that the sensor on the dipole speaker has a sensitivity of $2.44mVm^{-1}s^{-2}$ and this sensitivity is $2.66mVm^{-1}s^{-2}$ for the monopole speaker. This was found after a $20Hz$ sine was given as input to the system and the output from the accelerometer was measured. It then can be calculated what the voltage to acceleration ratio from the accelerometer is.

Accelerometer noise

The accelerometer noise is another important noise source that will be discussed. The fundamental noise limit of a piezoelectric accelerometer is generally determined by the noise of the piezoelectric transducer [15]. Piezoelectric transducers consist of two parts [15]:

- A mechanical damped harmonic oscillator.
- An electrical piezoelectric element.

These two parts contribute to the noise where a distinction can be made between the following:

- Thermo-mechanical noise (Brownian noise).
- Thermo-electrical noise.

Oftentimes, thermo-electrical noise can be neglected [15]. A thermo-mechanical noise model can be obtained from analysis based on the mechanism of Brownian Motion (or Wiener process). The Brownian motion analysis can be done by taking the integral of standard Gaussian white noise. This is more commonly known as the Wiener process. Similarly, the Brownian noise model can be obtained by multiplying the white noise model with $1/s$ (with $s = j\omega$) in the frequency domain. This can be done because a multiplication by $1/s$ in the frequency domain is equivalent to an integral in the time domain. The result of this noise model is shown in Figure 5.4. Several studies mention that common spectral behaviour of noise was found in the sense that $1/f$ noise dominates at low frequencies [9]. The obtained results seem to be following this observation. Hence, a new model is made where it is decided that white noise will be of relevance for the lower frequencies where $1/f$ noise dominates. Brown noise will be relevant for the higher frequencies in the band from $20-300Hz$. The model is designed in this way such that a more accurate fit could be made of the measured noise data concerning the modelled noise. The result of this combination of noise can be seen in Figure 5.4.

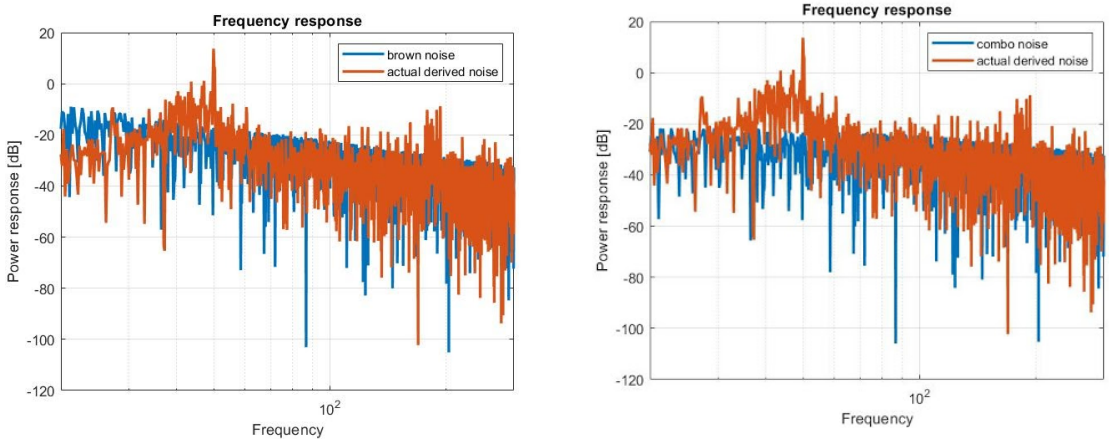

(a) Measured accelerometer noise and modelled accelerometer noise using a Brownian noise model.

(b) Measured accelerometer noise and modelled accelerometer noise using a combination noise model consisting of Brownian noise and Gaussian white noise

Figure 5.4: Accelerometer noise model, for the Brownian noise and combination noise respectively.

The obtained noise model, which will be called N_M, will be used in the transfer function $S_M(s)$ which represents the propagation of N_M through the system. The transfer function is given by Equation (4.10) and the result of the added noise source N_m on the system is shown in Figure 5.5.

Alternatives

As it is not the scope of this project to look into other solutions for measuring the speaker's output, only suggestions will be given. One of these suggestions is a light-based sensor. Pointing a laser on the speaker's cone (potentially on the back-side) is a method which uses the phase difference a first sent and then received light-pulse to calculate the distance from the cone to the sensor [26]. Because the speed of light is approximately $3.0x10^8 m/s$, a very high sampling frequency has to be used to create high-resolution data. A small disadvantage could be that another additional micro-controller would have to be used to create for instance a voltage that corresponds with some factor to the acceleration of the cone. Another alternative could be a microphone. The speaker is producing sound and it would thus be a logical step to measure this sound inversely the way it was produced. The implementation of the accelerometer itself can also be altered. In Chapter 2, an example product from PirateLogic was mentioned [19]. This product uses an accelerometer not on the front of the cone but on the back. It is also possible to measure the acceleration by the induced voltages on the voice coil [28]. These alternatives do not directly offer values with relation to the acceleration. They should be integrated over time once when they measure speed and twice when they measure distance to provide a voltage per acceleration signal.

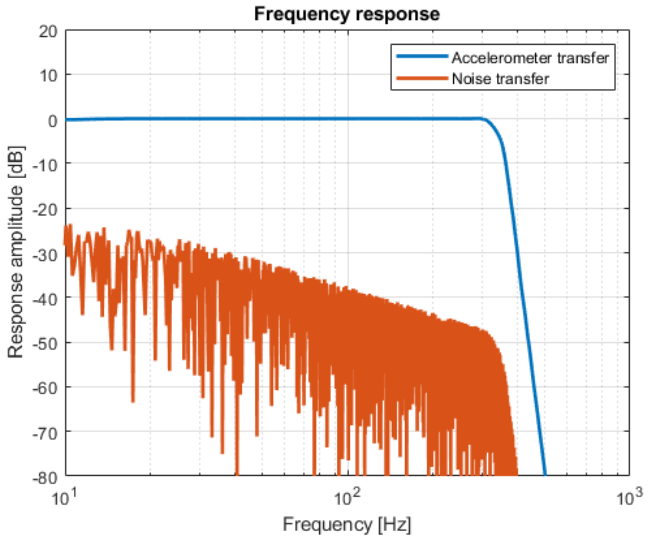

Figure 5.5: Frequency response of the transfer function from Equation 4.10 and when accelerometer noise is added to the system.

Conclusion
There are multiple solutions for generating feedback. In the end, it seems to be a more accurate method to use information based on acceleration because this is proportional to the current that is driving the speaker's cone. The way an accelerometer is used may be improved, however, in order to minimize negative effects on the outcome. One of the future projects suggested is doing research on the provided possibilities above and how they compare to other of providing the feedback loop.

5.2.2. Feedback loop subtraction

The control system is making use of negative feedback which means that feedback f provided by the accelerometer needs to be subtracted from the input signal i. The subtracted signal, also known as the error signal e, is amplified and fed back into the plant such that the error will be reduced due to this continuously repeating cycle. Contrary to the title /subject of this project, the implementation of this subtraction has been chosen to be analogue instead of digital. The main reason for this analogue implementation is that the so-called error signal e is very small and can take on values in the order of nano-volts. These voltages of the error signal can be so small that quantization errors will have large effects. Besides, the error signal will most likely be represented by only a small fraction of the available resolution in the digital domain. Quantization errors can take place when the signal has very small values comparable with a magnitude of $200nV$, which is deduced in Subsection 5.6.1. The analogue solution is to subtract the feedback signal from the input signal using an opamp circuit. Then, a component M will be used to amplify this signal such that the error signal e will be represented by a more relevant fraction of the available bits in the digital system. The simplest solution would be a differential amplifier, but some other solutions are given and compared as well. The desired outcome of the subtraction is given by Equation (5.1) in which a is an amplification factor.

$$V_{out} = V_{error} = a \times (V_{input} - V_{feedback}) \tag{5.1}$$

differential amplifier
The differential amplifier is given in Figure 5.6a. This differential opamp circuit has an output voltage given by Equation (5.1) ($a = 1$). This is the ideal output voltage. In reality, the output due to common-mode voltage on the input and the corresponding CMRR (common-mode rejection ratio) has to be taken into account. Besides, the opamp has an offset voltage and an offset current leading to a different output voltage as expected in comparison with the ideal situation given by Equation (5.1). This makes Equation (5.1) an equation for the ideal situation rather than the realistic situation. The influences of these non-idealities and what these non-idealities are, are discussed below.

The output voltage of this circuit, based on a linearly increasing common-mode input voltage (V_{cm}), is shown in Figure 5.7. The common-mode gain of this circuit is shown in Figure 5.8. The common-mode gain

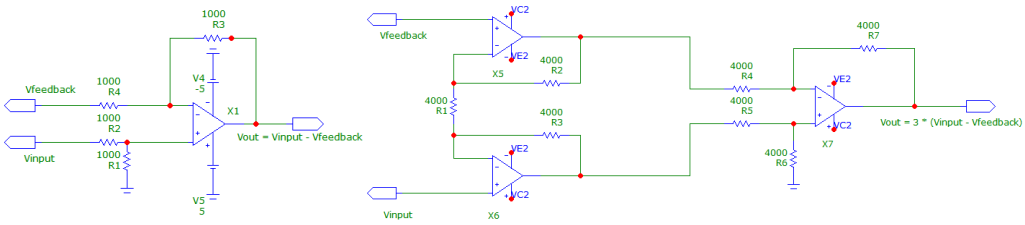

(a) Differential amplifier

(b) instrumentation amplifier

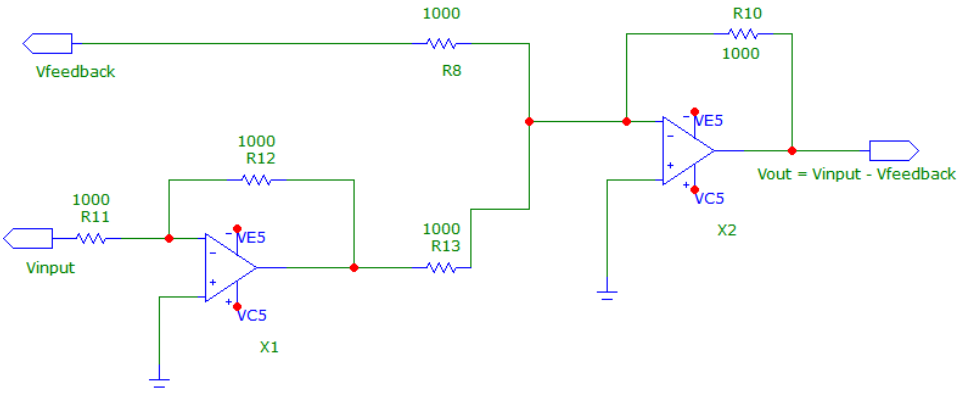

(c) Alternative method

Figure 5.6: Three discussed amplifier circuits for the adder (subtraction)

is already very low (less than $-120dB$) and can be reduced even further using an instrumentation amplifier circuit which has more potential beneficial aspects. Those will be described in the section about the instrumentation amplifier, Section 5.2.2.2.

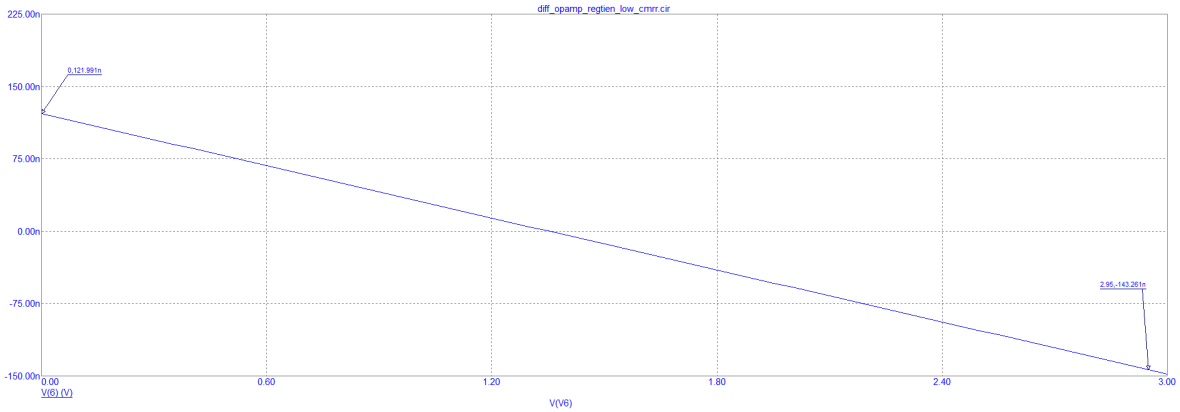

Figure 5.7: Common mode output voltage of the differential amplifier due to common mode input voltage. $V(V6) = V_{cm}, V(6) = V_{out}$

Using Microcap 12 [24], the noise of the circuit output due to offset voltage and offset current is shown in Figure 5.9. This noise has an over-time measured average of about $122nV$, which is less than the relevant $200nV$ described in Section 5.6.1. When this noise is being amplified in a component M, however, it becomes relevant to the system because it is then detected by the ADC of the ADAU, which is not desired. In these simulations, the OPA177 opamp has been used. This is a high-precision opamp and it is used in all the simulations executed for the other amplifier circuits as well. Better results may be obtained by using another amplifier.

Instrumentation amplifier

The CMRR of the differential amplifier already looks quite promising but can be improved. A method of increasing the CMRR is offered by an instrumentation amplifier. This circuit is obtained from the book Elec-

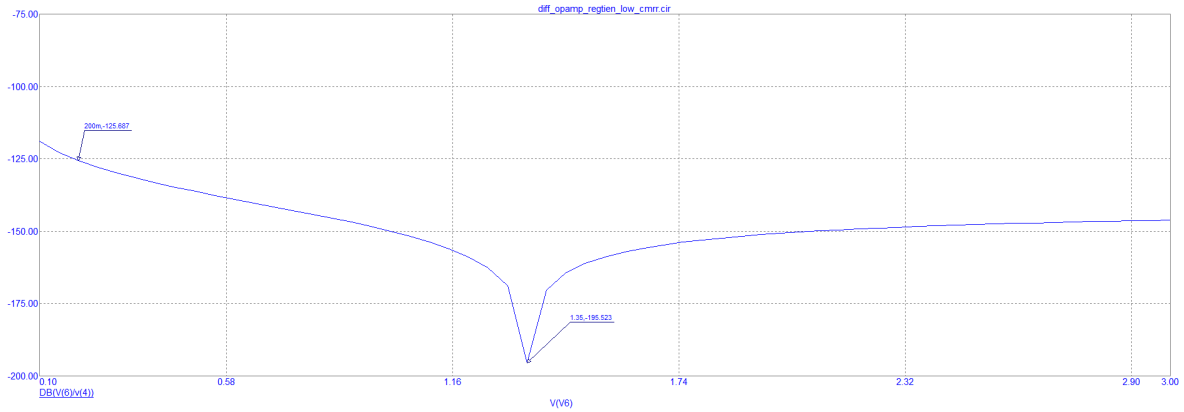

Figure 5.8: Common mode gain behaviour of the differential amplifier. $V(V6) = V(4) = V_{cm}, V(6) = V_{out}$

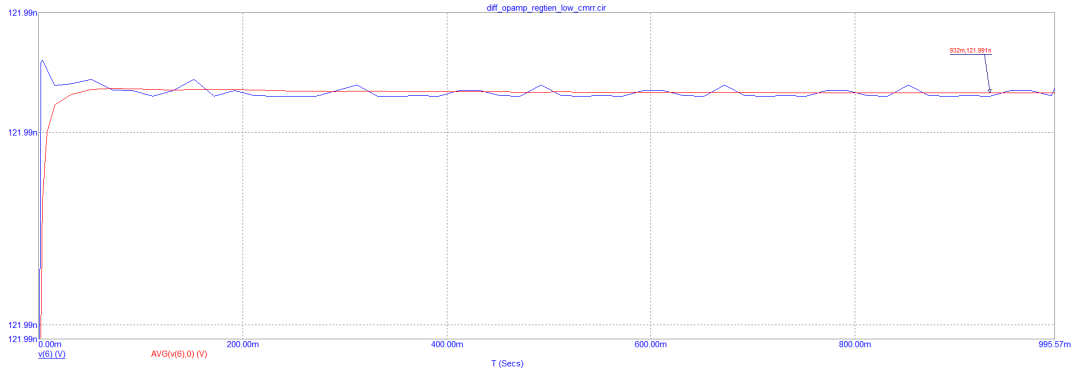

Figure 5.9: Output noise of the differential opamp circuit, averaged over time $V(6) = V_{out}$

tronic Instrumentation [20] and shown in Figure 5.6b. The common-mode gain from the instrumentation amplifier circuit (Figure 5.11) is the same when compared to the common-mode gain from the differential amplifier circuit (Figure 5.8) but the circuit gain from the instrumentation amplifier is (at least) three times larger ($9.54dB$) which means an even higher CMRR for the instrumentation amplifier circuit in comparison with the differential amplifier circuit. For the instrumentation opamp circuit to work, all the resistors should have the same value as R_2, except for resistor R_1. The circuit gain A_d is then determined as in Equation (5.2).

$$A_d = 1 + \frac{R_2}{R_1} \tag{5.2}$$

Because the CMRR is determined by Equation (5.3), the CMRR increases when the gain of the circuit increases. A_d is the circuit gain and A_c is the common-mode gain. The common-mode gain is the gain found in Figure 5.11. The common-mode gain, however, does not change when the circuit gain, given by Equation (5.2), is changed. By adding this gain, another amplifier would not have to be added as is discussed in Section 5.6.2. Besides, by adding this gain, the CMRR and the SNR (signal to noise ratio) would be improved because noise induced in the circuit would not be amplified.

$$CMRR = \frac{A_d}{A_c} \tag{5.3}$$

The output voltage of this circuit, based on a linearly increasing common-mode input voltage, is represented by Figure 5.10. The common-mode gain is shown in Figure 5.11. Changing the circuit gain from Equation (5.2) will not influence the results given by these figures, which is the desired effect as discussed above.

The voltage on the circuit output, due to offset voltage and offset current, is shown in Figure 5.12. This output voltage has an over-time measured average of about $122nV$, which is less than the relevant $200nV$

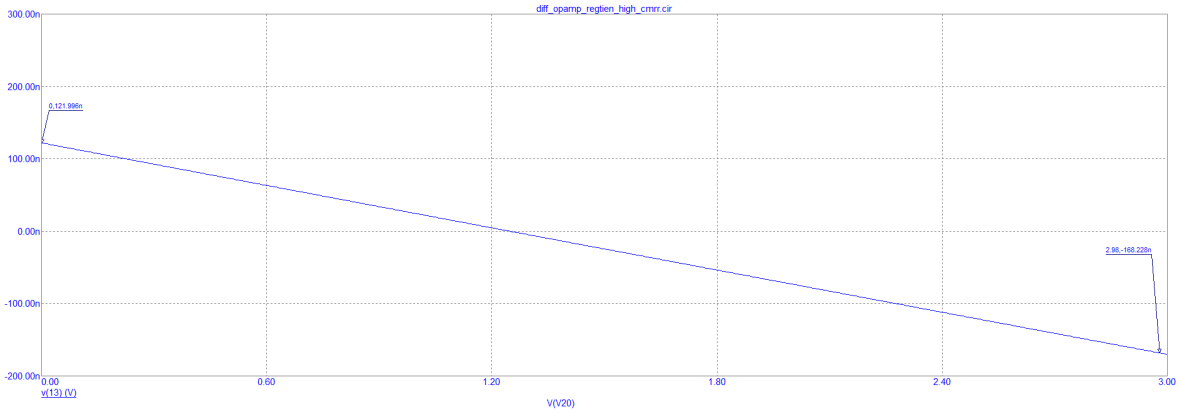

Figure 5.10: Common mode output voltage of the instr. differential amplifier due to common mode input voltage. $V(V20) = V_{cm}, V(13) = V_{out}$

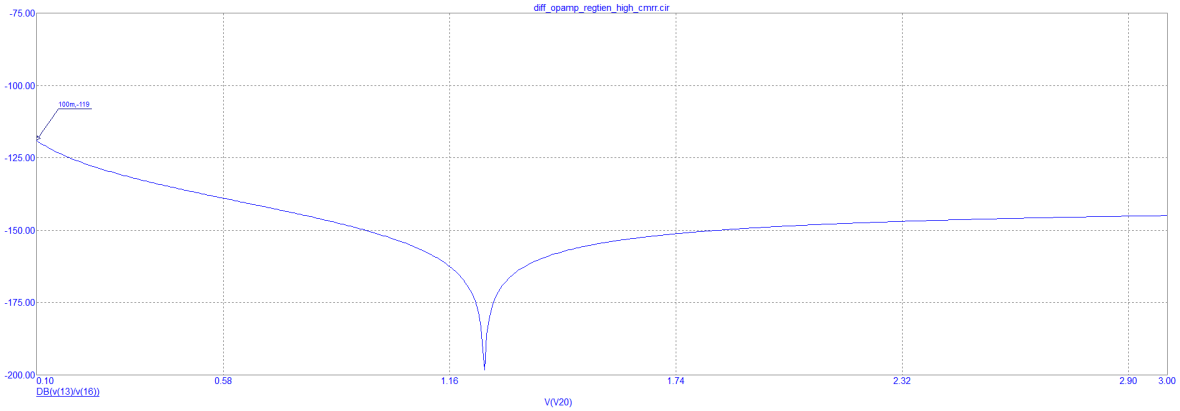

Figure 5.11: Common mode gain behaviour of the instr. differential amplifier. $V(V20) = V(16) = V_{cm}, V(13) = V_{out}$

but can still have an influence. The noise for the same circuit with the gain set to, for example, $30dB$ leads to the same output voltage as the circuit without the $30dB$ gain. The $30dB$ gain is rather randomly chosen but shows that there is no effect. In Appendix B.2 the confirmation is shown.

Using SLiCAP [17], a noise equation for this circuit was obtained. When approximated and rewritten, this noise equation becomes equal to Equation (5.4) with S being the output noise power spectral density given in $\frac{V^2}{Hz}$. Appendix B.1 can be looked into for details on the full, original equation. The approximation is based on neglecting thermal noise [15] and setting all resistors (except resistor R_1) equal to R_2. In this Equation, S_{i1}, S_{i2}, S_{i3} are the input noise currents of the three opamps given by the circuit.

$$S \approx R_2^2(S_{i1} + S_{i2} + 3S_{i3}) \tag{5.4}$$

It is good to notice, that the output noise given by Equation (5.4) is not depending on R_1 which is used to set the gain of the circuit according to Equation (5.2). This suggests that the error signal e can be amplified without the noise being amplified such that the SNR of this amplifier circuit is increased.

Alternative (non-differential) amplifier

There are setups that make use of a non-differential amplifier as for example the one that is given in Figure 5.6c. When a common-mode input signal is offered to this circuit, it can be seen from Figure 5.13 that there still is an output voltage present but this is due to offset voltages and currents on the amplifiers. Because the positive inputs of both amplifiers in this circuit have been connected to ground, the amplifiers will try to drive their inverted input to ground. The common-mode input voltage of both amplifiers will be zero, hence, any common-mode gain will add gain to a common-mode input of zero volt which has no effect. The output voltage that is still present has a value of about $60nV$ on an over-time average which is low compared to the

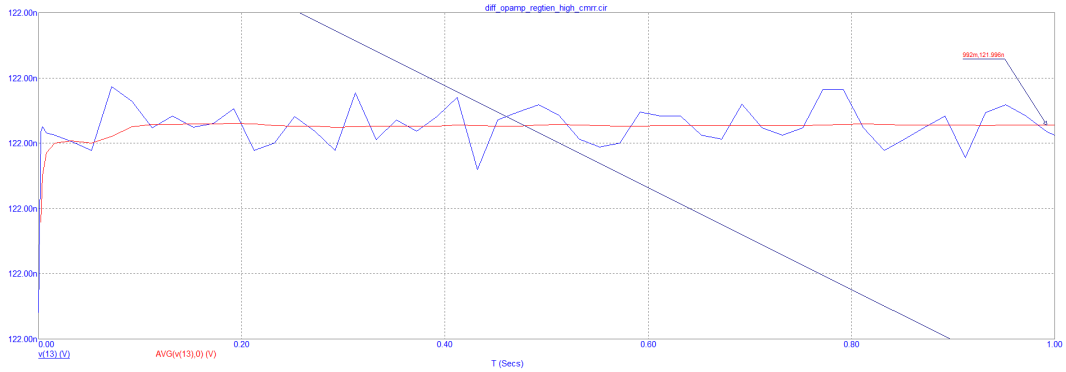

Figure 5.12: Output noise of the instr. differential opamp circuit, averaged over time. $V(13) = V_{out}$

$200nV$ sensitivity of the ADC. Moreover, by adding gain to this circuit, the circuit gain will increase but this output voltage due to the offset will not. Adding gain to this circuit, however, will have negative effects as will be discussed below.

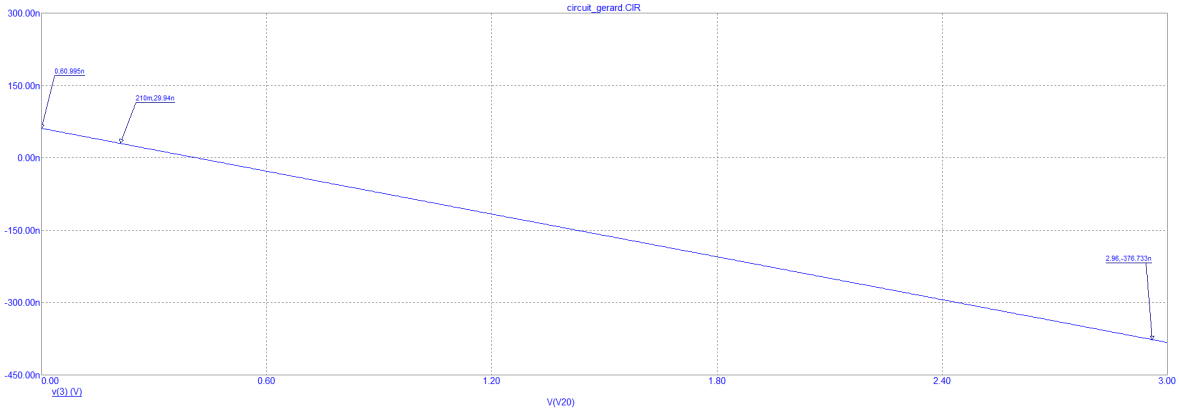

Figure 5.13: Common mode output voltage of the alternative amplifier due to common mode input voltage. $V(V20) = V_{cm}, V(3) = V_{out}$

The noise induced by the circuit is the main issue of this circuit. Just as is done for the instrumentation amplifier circuit in Equation (5.4), the noise of this alternative circuit is described in an equation provided by SLiCAP [17]. This equation can be simplified to Equation (5.5). This is done by setting all resistors, except for resistor R_{10}, equal to R. In addition thermal noise components have been neglected. Resistor R_{10} is set equal to aR in which a is the gain factor of the circuit. The original equation can once again be found in Appendix B.1. Equation (5.6) gives the output noise power for a $0dB$ gain at which $a = 1$, in $\frac{V^2}{Hz}$.

$$S \approx \frac{a^2 S_{i1}}{R^2} + a^2 R^2 S_{i2} + 4a^2 S_{v1} + (1+2a)^2 S_{v2} \tag{5.5}$$

$$S \approx \frac{S_{i1}}{R^2} + R^2 S_{i2} + 4S_{v1} + 9S_{v2} \tag{5.6}$$

5.2.3. Conclusion

From all the circuits given, a phase delay in the order of milli-degrees was noticed. A phase delay with this size is so small that a conclusion should not be based on this matter when the specifications require a maximum phase delay of 45° for the whole system.
The instrumentation opamp circuit has the same output voltage due to offset currents and offset voltages as the differential opamp circuit but the CMRR of the instrumentation amplifier circuit is larger. The gain of the instrumentation opamp circuit, is at least 3 times larger ($9.5dB$) by default, meaning that the instrumentation opamp circuit without additional gain already has an advantage compared to the differential opamp circuit.

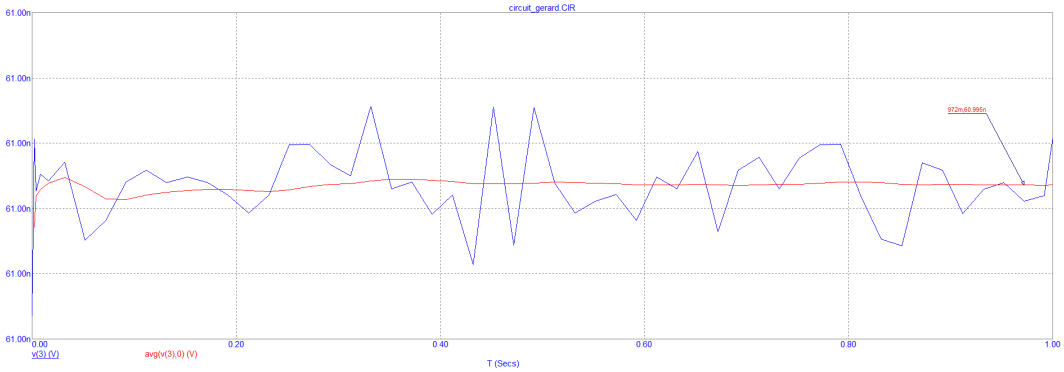

Figure 5.14: Output noise of the alternative opamp circuit, averaged over time. $V(3) = V_{out}$

The CMRR of the instrumentation amplifier circuit may be disadvantageous for this circuit in comparison to the alternative circuit. However, the noise from the inputs of the opamps used in these circuits, in combination with the possibility of adding gain a to the circuit, are a deal breaker for the alternative circuit.
When for both circuits the same opamps and resistor values are used and it is assumed that the alternative circuit would not offer gain as this would make the output noise value even higher, it can be found for which value of S_v they would have the same noise output power. To calculate this, Equations (5.4) and (5.6) are equated to each-other under the given assumptions. It can be concluded that $S_v \approx 0.31 S_i$ when both circuits would have the same noise output power. If such an opamp would be used, it still is suggested to use the instrumentation amplifier circuit for SNR reasons. In the comparison made, the instrumentation amplifier would already have a $9.54dB$ SNR gain advantage over the alternative amplifier circuit. This is without gain added. By adding gain, the SNR of the instrumentation amplifier circuit would increase with a steeper slope than the SNR of the alternative circuit would. This is due to the output noise power of the alternative circuit which increases when the gain increases.

5.3. Voltage to current amplifier

The voltage to current amplifier will not be thoroughly discussed in this report since the scope of this thesis is about the control system. The voltage to current amplifier is part of the overall project but is handled by another team. This is why only the results and useful characteristics of the amplifier will be shown in this section. For the full derivation and theory coming with designing the voltage to current amplifier, it is advised to take a look at the report of this subgroup [1].

5.3.1. Amplifier noise and delay

Amplifier noise could be a potential detrimental noise source in the system. The noise derivations have been done by the amplifier subgroup [1]. The noise data provided by them will be of interest for this section, and this data will be used to make a noise model. Moreover, the transfer of the noise with respect to the output will be investigated.

The obtained amplifier noise model (N_k) is shown in Figure 5.15, this model will be used in the transfer function $S_k(s)$ which represents the propagation of N_k through the system. The transfer function is given by Equation (4.9) and the result of the added noise source N_k on the system is shown in Figure 5.16.

According to the amplifier subgroup, a minimum voltage to voltage gain of 30 can be expected to be provided by the amplifier. The amplifier is thus modelled in the control system design as a frequency independent amplifier with a voltage to voltage gain of 30. Besides this, the amplifier inflicts a delay of $30\mu s$ to the system [1]. This delay could potentially contribute to the system becoming unstable due to a too large delay in the system.

5.4. System gain

The whole system, from input to output is desired to have a gain. The VCCS amplifier in the system is present to provide loop-gain and to drive the speaker but, is not addressed further in this report. This report focuses

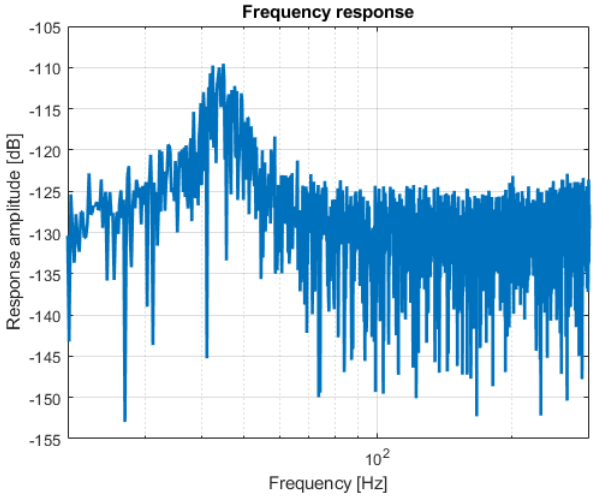

Figure 5.15: Voltage to current amplifier noise

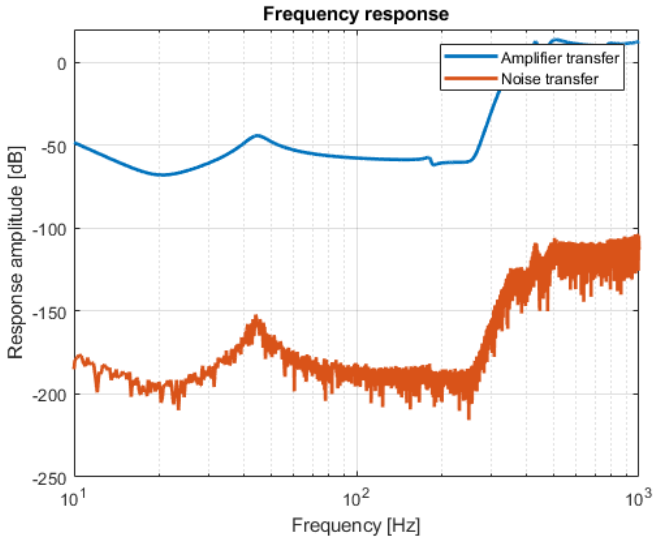

Figure 5.16: Frequency response of the transfer function from Equation (4.9) and when amplifier noise is added to the system.

on controlling the system, of which this amplifier is a part, using a feedback loop. A unity gain in the feedback path in a control system causes the gain of the system to be $0dB$, which is not what is desired for this specific system. In order to have gain, the feedback loop should not deliver unity gain feedback as is explained in Section 4.4. This is where the P component, given in Figure 4.6, comes into play. The signal coming from the sensor /accelerometer ($A(s)$), that is seen as the output from the system (y) in this system, tends to have a $0dB$ gain factor on the input signal i from the system, due to the feedback loop. Component P sets the gain of the closed loop system when it changes this feedback signal with a factor of $\frac{1}{30}$ (with 30 being the desired gain). Initially, the system gain was set by K when there was no feedback and control system. Now that there is a feedback loop, a gain is still desired but no longer depending on this component K. Given that the gain of the closed-loop system should be $30 = 29.54dB$ according to the requirements 3, P should be set equal to $\frac{1}{30}$.

Block P represents a simple linear amplifier. With a simple voltage divider, the desired amplification of $\frac{1}{30}$ can be obtained. One such voltage divider circuit is given in Figure 5.17. The designed voltage divider contains just two resistors but also an opamp to create a lower load connected to the voltage divider. The two resistors given in the schematic are R_1 and R_2. They should have a ratio as given in Equation (5.7). When the gain is set to have a gain of $29.54dB = 30$, the values of R_1 and R_2 can be chosen to have the ratio $R_1 = 29R_2$ according to Equation (5.7).

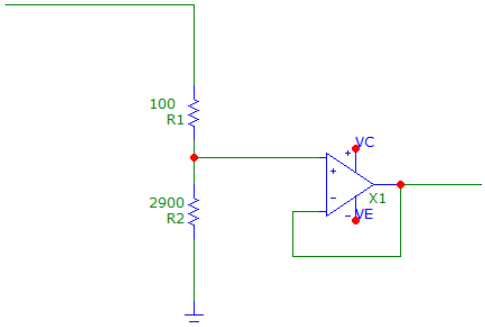

Figure 5.17: Voltage amplifier for component P, system gain

$$R_2 = R_1(30-1) = R_1 \times 29 \tag{5.7}$$

When the feedback signal is subtracted from the input signal using an instrumentation amplifier, the amplifier in the voltage divider design would not be needed. This is due to the fact that the inputs of the instrumentation amplifier are directly subjected to opamps. The latter statement is beneficial as an additional opamp would again have a noise current, a noise voltage, offset current and offset voltage.
The system gain component (P) is designed as a frequency-independent element. This is due to the fact that the gain provided to the output signal should be frequency independent. The controller is set in place to handle frequency-specific characteristics such as filtering or adding loop-gain. The multiplication factor of P will be smaller than 1 as it is a division of 1 over the desired gain.

5.5. Controller

The controller can be seen as the centre of the control system and will add frequency-dependent loop-gain to the system in order to influence the loop-gain of the system in a desirable way. It will also filter out the undesired and destructive responses at some frequencies in the system to make sure the system is stable. To be able to easily do the corresponding signal processing, the earlier mentioned ADAU1777 chip [4] will be used. The reason this chip is used is that it has very low latency but can still perform some useful signal processing such as adding gain and different types of filters. Three possible controller designs will be shown in this section and two ways to filter out undesired frequencies outside of the desired pass-band will be given. Since the ADAU is a digital chip, ADCs and DACs are required to convert from the analog to the digital domain and vice versa. These conversions will result in quantization noise and this will be modelled to be able to check its influence on the system later on. Before the controller and its functionalities will be described, the feedback loop will be closed and several components will have some initial values to be able to qualitatively describe the controllers influence on the system.

5.5.1. Initial system

The monopole filter will be used as an example for describing the controller. Its frequency response can be found in Figure 5.1. The negative feedback loop (shown in Figure 4.6) will be closed and some components will have a transfer different than unity gain. First of all, the system gain P will have a gain of $\frac{1}{30}$ to make sure that the required input to output gain of $30 = 29.54dB$ is achieved. Since input to output gain will result in a decrease of available loop-gain, it was decided to put the voltage amplifier M to a voltage to voltage gain of 30 to compensate for this. The voltage to current amplifier designed by the other sub-group [1] has a minimum gain of 30 (voltage to voltage) and it is thus modelled like a voltage to voltage gain of 30 in the system. Finally, the speaker $G(s)$ is modelled as the frequency response given in Figure 5.1. After implementing all these components in the system, the transfer function and phase response of the system as a whole will look like the blue plot given in Figure 5.18, for the monopole speaker. A similar plot for the dipole speaker can be found in Figure E.1. The green dotted lines indicate the pass-band which should at least be controlled.

At first, these results may look like an adequate result and not too many adjustments should be done to optimize these systems. These systems, however, are not stable at all. The loop-gain in the system is also not constant and is thus not used to its full potential. How this system can be stabilized and optimized will be explained in the following subsections.

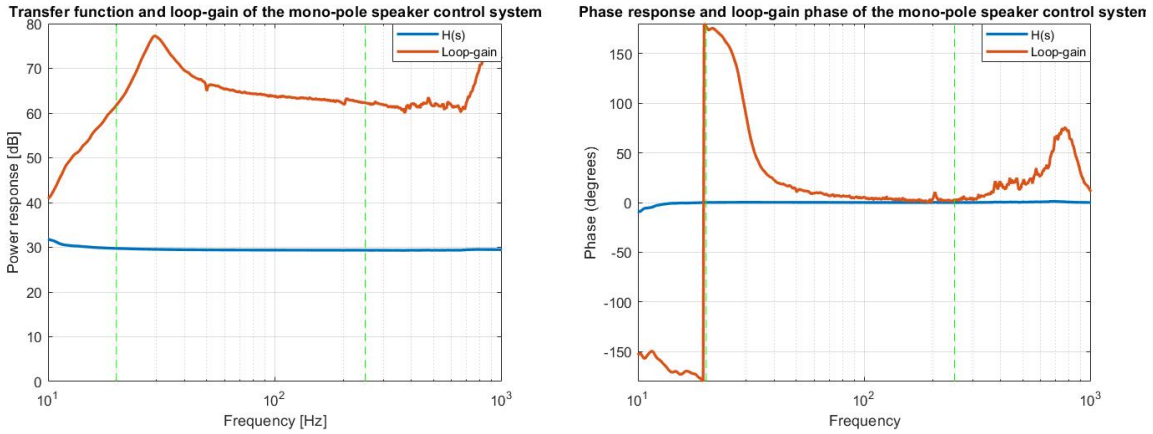

(a) The frequency response of the system.

(b) The phase response of the system.

Figure 5.18: Initial system response without any signal processing done in the controller.

To be able to compare the different implementations of the controller, all configurations will be provided with the maximum amount of loop-gain that would still lead to a stable system. A stable system is defined as a system with a Phase Margin (PM) of at least 45, which is a common rule of thumb for constructing a stable system [23]. Besides this, the Nyquist plot should not encircle the -1 point to ensure stability [10]. This loop-gain will be added in the analogue voltage amplifier which will be discussed in Section 5.6.

5.5.2. Filters

As mentioned before, filters are used to suppress the loop-gain at frequencies for which the speaker and accelerometer response is large and outside of the frequency band of interest. As can be seen from the red plot in Figure 5.18 for the monopole speaker (Figure E.1, for the dipole speaker), the loop gain is inconsistent across the frequency band of interest. This indicates that the loop-gain might not be used to its full potential. Besides, the loop-gain is reaching to $80dB$ at some points which may cause the system to become unstable. Dealing with high loop-gain at the frequencies outside the pass-band can be done with filters. An important note on designing the filters for the motional feedback control is that the quality of the pass-band is more important than the width of the pass-band. In other words, the minimum controlled pass-band is the one as given in the programme of requirements but controlling a wider frequency range is not a problem as long as this does not make the system unstable and the pass-band remains flat. The filters can thus be placed well outside of the minimum required controlled pass-band if this increases the system performance in the pass-band.

The types of filters used to do this are Butterworth filters. The main reason for choosing Butterworth filters is that they show little ripple inside the pass-band compared to other filter types [6]. This comes, however, at the cost of a not steeply decreasing slope outside of the pass-band compared to other filter types [6]. This will not be a major problem since a strict pass-band is not required for this system. Filtering the desired pass-band can be done using low- and high-pass filters. Notch filters can also be used to solely filter out the peaks occurring at frequencies $2000Hz$ and higher in the speaker response.

Filtering frequencies below pass-band

For suppressing the frequencies below the desired pass-band, a high-pass filter will be used. The reason for this is that the sole purpose of filtering out these frequencies is to make sure that the system will not oscillate at very low frequencies when minor fluctuations occur in the speaker. If these frequencies would not be filtered out, these oscillations will dampen out very slowly since the control system will keep controlling at these frequencies thus not allowing them to dampen out. For this purpose, a low order high-pass filter can be used and the results after implementing this in the system for the monopole speaker can be found in Figure 5.19. Similar results for the dipole speaker can be found in Figure E.2. Since the plots will now represent a stable system, the loop-gain is very low ($0dB$) compared to Figure 5.18. The only way to make the system with solely the high-pass filter stable is by taking down the loop-gain drastically. As a result, the feedback system

will not control the output and also not increase the response performance. What can be concluded from this plot is that the high-pass filter does filter out low frequencies. As can also be seen from these plots, the phase of the loop gain is altered after adding these filters. This will prove not to be a problem later on and will be corrected for by the control system when adding loop-gain becomes possible when the controllers are put into place.

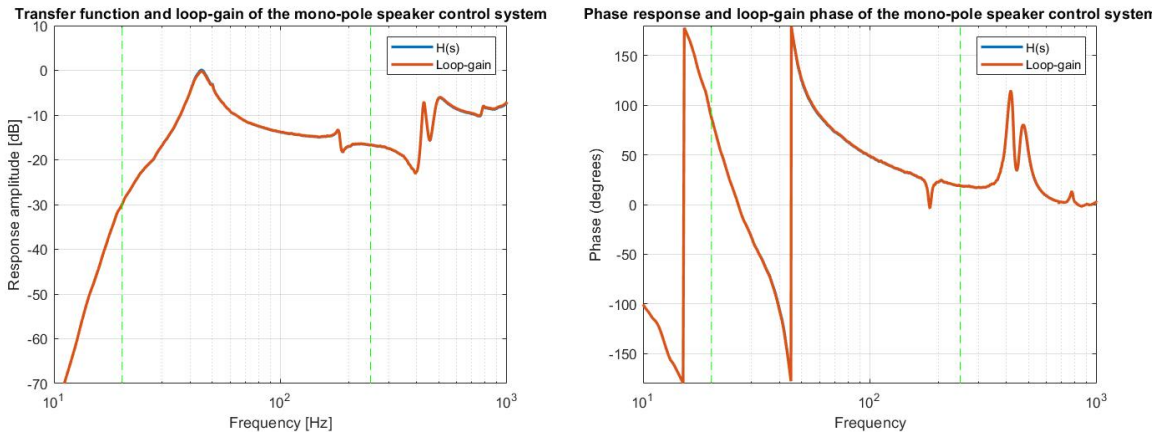

(a) The frequency response of the system.

(b) The phase response of the system.

Figure 5.19: The system response after adding a simple high-pass filter in the controller. (The transfer function and the loop-gain are nearly the same and are thus plotted over each other.)

The stability problems, leading to a very low achievable loop-gain, occur due to fluctuations at higher frequencies. These fluctuations should thus be accounted for using filters. The two options of filtering that will be covered here are using a high-order low pass filter or a collection of notch filters at the designated undesired peaks in the loop-gain. The design and pros and cons of these filters will now be described in more detail.

Filtering frequencies above the pass-band with a low-pass filter

This approach is similar to the approach for designing the high-pass filter which filters out the lower frequencies. The major difference is that this filter requires a higher order to successfully do its work. The reason for this is that it should suppress the high peaks found in the speaker response above the pass-band. A major downside coming with using high order low-pass filters is that the phase will be greatly influenced which may cause instability in the system. This shift in phase can be accommodated for by the control system but it also brings another problem to the table. When the loop-gain decreases steeply and the phase is also changing rapidly close to this cut-off frequency, this may result in a small peak just before the transfer of the system starts decreasing. In other words, when using a high order low-pass filter, a small peak can be found just before the frequency response of the control system starts decreasing. This also leads to instability in the system since the frequencies around this cut-off frequency will be present very close to the -1 point in the Nyquist plot.The magnitude of this peak is greatly dependent on the frequencies at which the filter is placed. To be more specific, the filter should be placed at the frequencies where the speaker response is low in magnitude, to minimize the magnitude of the peak. A possible reason for this is that at these frequencies the loop-gain will not only decrease due to the filters but also because of the decreasing frequency response of the speaker. A more robust proof of this is, however, yet to be found and further research regarding this exact placement is still necessary. When placing the filter with high enough order and at the correct frequency, the results will be as given in Figure 5.20, for the monopole speaker system. Similar results for the dipole speaker can be found in Figure E.3. As can be seen in the figures, the loop-gain of this system compared to the loop-gain with only the high-pass filter in the system could be increased to $10dB$ before instability occurred. This is still far from enough to be able to usefully control the speaker response but does show that adding this low-pass filter to the system will increase the stability of the system. The controllers presented later on will make it possible to further increase this loop-gain. As can also be seen in the figures, the low-pass filters add a severe phase change to the loop-gain. These phase changes can be handled by the control system but at some point,

increasing the order of the filters will result in an unstable system.

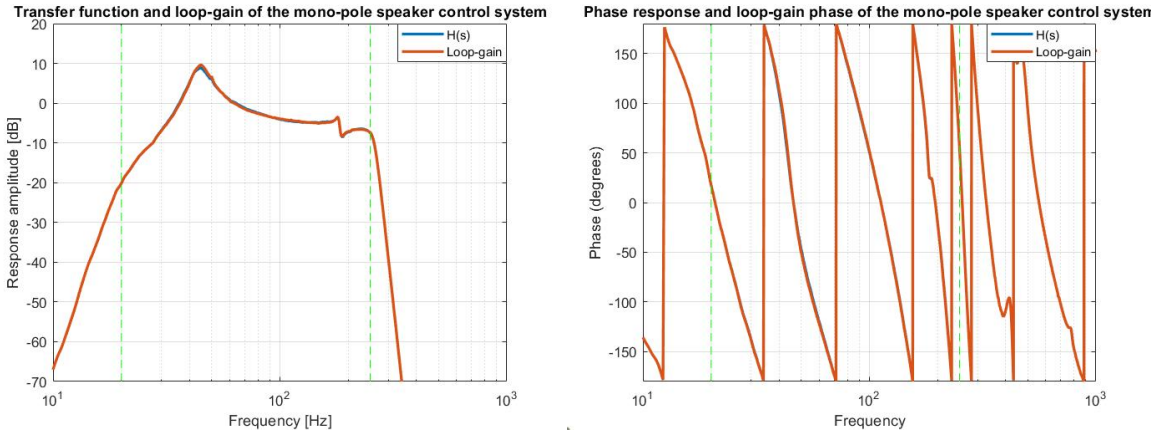

(a) The frequency response of the system.

(b) The phase response of the system.

Figure 5.20: The system response after adding a simple high-pass filter and a high order low pass filter in the controller.

Filtering frequencies above pass-band with notch filters

Another way to filter out unwanted frequencies is by adding notch filters at the high peaks in the loop-gain occurring at higher frequencies. By using notch filters, the phase response inside the pass-band will be hardly influenced and this should thus not result in the potential stability issues that come with implementing a high order low-pass filter. By placing these notch filters at peaks, which occur in the frequency response of the speaker, the loop-gain at these frequencies will be suppressed. When using notch filters instead of a low-pass filter, only the response at certain frequencies will be suppressed and the leftover frequencies will be controlled by the control system. This will not be a problem since the quality of the pass-band is important and not the width of it. The response of the control system, with the notch filter implemented instead of the low-pass filter, can be found in Figure 5.21. The figure shows a loop-gain increase of $11dB$ compared to the system containing the high order low-pass filter 5.20, indicating that using notch filters makes the system more stable. As can also be seen from the phase response of the system, the phase fluctuates less than for the high order low-pass filter thus having less potential to destabilize the system. An important reason for this is that the notch filter has a lower order than the high order low-pass filter. The pass-band is also much wider compared to the pass-band width when using a high order low-pass filter. A downside of using notch filters is that high frequencies ($5kHz$ and higher), which could occur in the system due to noise, will not be suppressed. Whether this will lead to problems is debatable since the speaker used is not designed to produce sound at these frequencies.

Which of the two filters to choose is dependent on what type of controller will be used. Choosing for the low-pass filter will make sure that frequencies above the cut-off frequency will be completely suppressed and will thus not have an influence on the stability. Choosing for the notch filters will result in less phase fluctuation in the loop-gain since notch filters only have an effect on the phase inside its stop-band. Notch filters also require a lower order to perform as desired function compared to the low-pass filter. Notch filters will thus be preferable due to the limited influence on the phase. They may, however, not be sufficient to suppress unstable frequencies above the minimum required pass-band, in which case a low-pass filter must be used.

Now that the filters have been designed, the performance of the system inside the pass-band can be increased. This can be done using controllers and three different types of the controller will be discussed in the following sub section.

5.5.3. pass-band controller

The three types of controllers that will be described in this subsection consist of a PD (Proportional-Derivative) controller, a controller which adds additional gain at frequencies for which the transfer function is not flat and

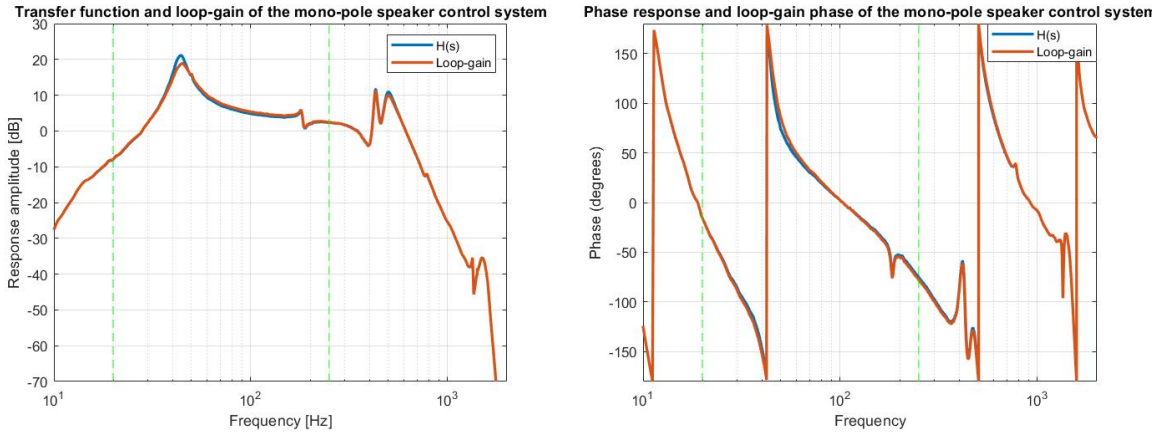

(a) The frequency response of the system.

(b) The phase response of the system.

Figure 5.21: The system response after adding a simple high-pass filter and a notch filter in the controller.

Controller	K_p	K_d	T_d
PD	$0.8K_u$	$\frac{K_u T_u}{10}$	$\frac{T_u}{8}$

Table 5.1: Ziegler-Nichols Tuning rules for a PD controller [10]

lastly, a controller which makes the loop-gain constant inside the pass-band. The design methodologies of these controllers will be given and the controller chosen for the control systems will be given. To be able to qualitatively compare the controllers, the loop-gain of the system will be increased until instability occurs. The controller which allows for the highest loop gain is the preferred controller design.

PD-controller

A first possible controller that can be used to optimize the system's performance is chosen to be one of the controllers covered in the systems and control course from the bachelor Electrical Engineering. These controllers are normally designed based on the step response of the system. Since DC is filtered out of the system, it doesn't make sense to analyse the step response and thus a delta spike could be used instead. Other characteristics that can be used are Gain margin and Phase margin. According to the book feedback control of dynamic systems [10], it is possible to use PID tuning rules [10] based on GM (Gain Margin), PM (Phase Margin) and the corresponding continuous oscillation frequency (W_{cg}). By using the MATLAB function "margin", the GM, PM and W_{cg} can be obtained. These parameters belong to the system that has not yet been provided with any form of PID (Proportional-Integral-Derivative) control.
Parameters for tuning a controller are ultimate gain (K_u) and ultimate period (P_u). The ultimate gain is the gain in the controller at which the system starts to oscillate with uniform oscillations (constant amplitude). The period of those uniform oscillations is also known as the ultimate period P_u. Increasing the ultimate gain to the uniform oscillation point can be a difficult task but finding the GM and the PM are rather simple to accomplish in comparison. The ultimate gain K_u can be set equal to the obtained GM. The ultimate period P_u is then equal to $\frac{2\pi}{W_{cg}}$.
With P_u and K_u known, tuning rules can be applied to set a form of PID control. As it is assumed that the system would not reach a steady-state error moment because DC signals are filtered out, the emphasis for this control is put on a PD controller. This form of control increases stability and decreases the maximum peak overshoot. Moreover, the PD controller decreases the settling time which is an advantageous factor for a system with rapidly changing input signals.

The default PD controller equation is given in Equation (5.8). The parameters of this equation can be obtained from the Ziegler-Nichols tuning parameters for a PD controller found from Table 5.1 [10]. With the correct parameters set, this PD controller can be implemented in the controller which is the DSP chip (ADAU1777).

$$H_{pd}(s) = K_p(1 + T_d S) \tag{5.8}$$

For this controller, the low-pass filter will be used to filter out higher frequencies instead of the notch filters. The reason for this is that the PD controller implements an increase of response amplitude for increasing frequencies. For higher frequencies this will lead to instabilities and a low-pass filter should be used to counteract on this behaviour of the PD controller. In Figure 5.22, the result from this PD controller can be seen after increasing the loop-gain until instability occurs. The response of this system is relatively flat inside the pass-band but at the very low frequencies a peak occurs. Adding more loop-gain to the controller will lead to a decrease of the Phase Margin due to phase fluctuations at $1909Hz$.

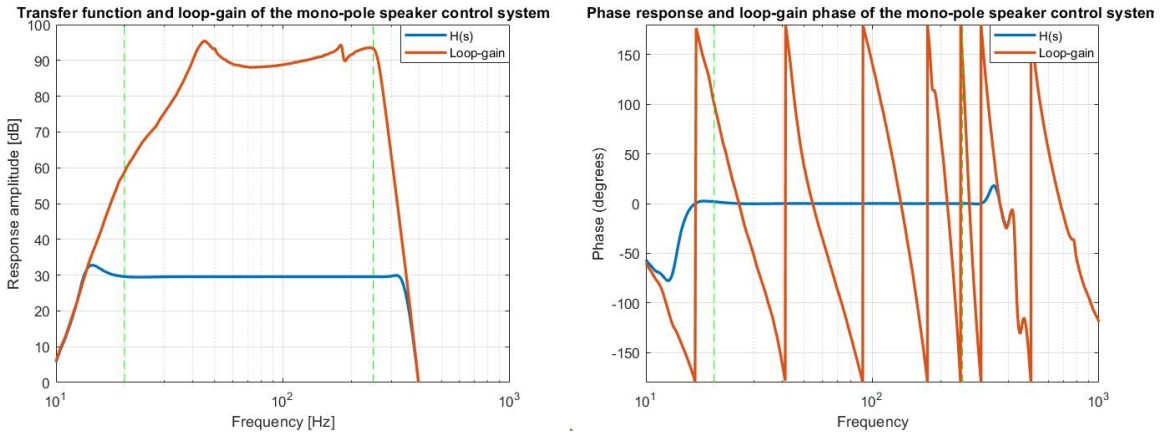

(a) The frequency response of the system.

(b) The phase response of the system.

Figure 5.22: The system response after adding a simple high-pass filter, a high order low pass filter and a PD controller to the controller.

Adding gain at specific frequencies

The control system should provide a transfer-function that is flat inside the pass-band with a gain of 30 = $29.54dB$, this is however not always the case for all frequencies. The reason for this is that there is not enough loop-gain present at these frequencies. This can be seen when looking at the transfer function given in Equation (5.9).

$$H(s) = \frac{M * D(s) * K * G(s)}{1 + M * D(s) * K * G(s) * P} \tag{5.9}$$

When M, $D(s)$, K and $G(s)$ implement enough loop-gain, the transfer function will converge to the outcome of Equation (5.10).

$$H(s) \approx \frac{1}{P} = 30 = 29.54dB \tag{5.10}$$

This equation indicates that at points where the response deviates from the $29.54dB$, the loop-gain is not enough and thus gain should be added. For this example, two major frequency bands in the transfer function that have these problems will be corrected by adding a specific amount of gain to the controller. The bands chosen are the ones just after the low-pass cut-off frequency and just before the high-pass cut-off frequency.

Adding specific gain at these frequencies can be done by adding band-pass filters with some gain to the controller at the required frequencies. The order of this band-pass filter should be chosen in such a way that it will not decrease the quality of the pass-band filtering done previously. If, for instance, the filter has an order 10 and a band-pass filter is added close to the cut-off frequency of this filter, the order of the band-pass filter should be at least 10 to not disturb the filters' performance. If such problems do not occur, the order of the band-pass filter should be chosen low to avoid a fluctuating phase. For this controller, the low-pass filter was chosen. The reason for this is that the controller itself will only compensate frequencies inside the pass-band and will not contribute to increasing stability outside of it. By using a low-pass filter, the uncontrolled frequencies can be filtered out and will thus not contribute to instability. Adding the previously described controller and increasing the loop-gain until instability occurs results in the system response for the monopole speaker are given in Figure 5.23.

The pass-band response using this controller is less flat than for the PD controller and this is the result of very little loop-gain being present. This limited amount of loop-gain originates from the fact that this specific gain addition implements instability to the system, especially regarding the phase of the system. This phase

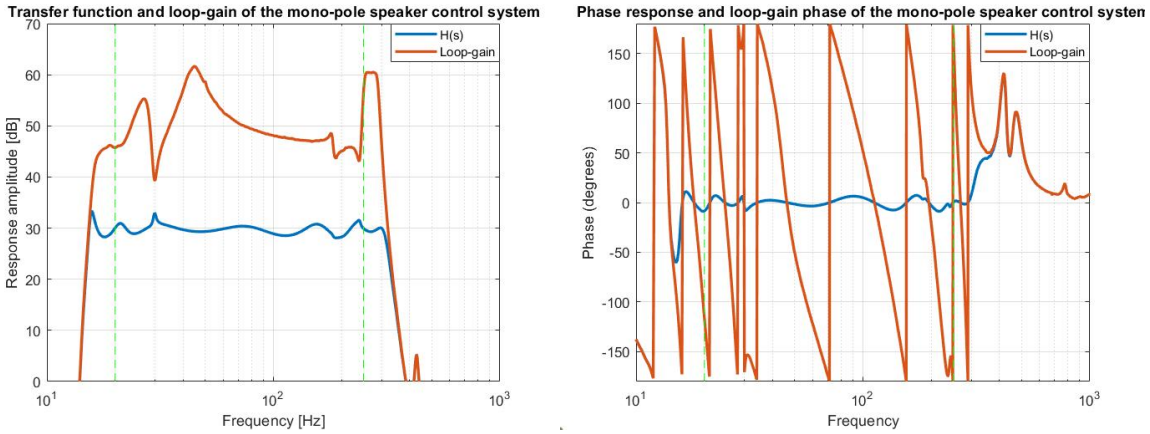

(a) The frequency response of the system.

(b) The phase response of the system.

Figure 5.23: The system response after adding a simple high-pass filter, a high order low-pass filter and adding extra at frequencies where the transfer function is not flat.

is also the reason why this system becomes unstable when more loop-gain is added. Just like for the PD controller, phase changes occurring at higher frequencies result in instability. Even though the principle of adding specific gain could be optimized, it was chosen not to do so since it seems very likely that the phase problems will even increase further.

Making the loop-gain constant inside the pass-band

Another possibility for the controller could be to add gain at certain frequencies inversely proportional to the speaker response. By doing this the response of the speaker will be compensated in such a way that the product will approximate to unity gain in the entire pass-band. The speaker model designed in sub Section 5.1.2 will be used to construct the controller. By using the inverse of the speaker as a controller, the loop-gain nearly becomes constant over the entire pass-band. This type of controller is based on an open-loop correction technique [7]. In this paper it is shown that adjusting the input signal with a function that is the inverse of the speaker response, the frequency spectrum of the output should, in theory, be close to constant. The closed-loop that will be added to this compensation technique (in this project) will even further improve the quality of the pass-band and will also decrease the influence of noise and non-linear distortion. Filtering in this controller will be done using notch filters. The reason for this is that the inverse model of the speaker will not only compensate frequencies inside the pass-band but also outside of it. Due to this, only a few peaks will remain present in the loop-gain due to resonances but these can be easily fixed using notch filters. By using notch filters instead of low-pass filters, the phase will not be influenced which will thus also contribute less to instability. Adding this controller to the system and maximizing the loop-gain results in the monopole speaker response given in Figure 5.24. Similar results for the dipole speaker system can be found in Figure E.4.

The quality in the pass-band of this controller is already much improved compared to previous controller designs. The main reason for this is that the loop-gain corresponding to this controller is constant throughout the pass-band. The system is even stable enough to implement even more loop-gain to the system (up to $160dB$ assuming no noise in the system) but this is not done since noise sources will become destructive at such a large loop-gain, this will be further discussed in 5.8. Instability occurring when adding more loop-gain (on top of $160dB$ loop-gain) originates from an unstable gain occurring at higher frequencies. Even though the speaker is not able to represent these frequencies, it could affect the stability of the system. The negative consequence originating from this controller is that its transfer is more complex than the ones from the other controllers. Since the ADAU uses digital signal processing this may not be a problem since precise signal processing can be done digitally. The ADAU is however designed for simple signal processing to guarantee low latency and implementing this controller could thus still give problems.

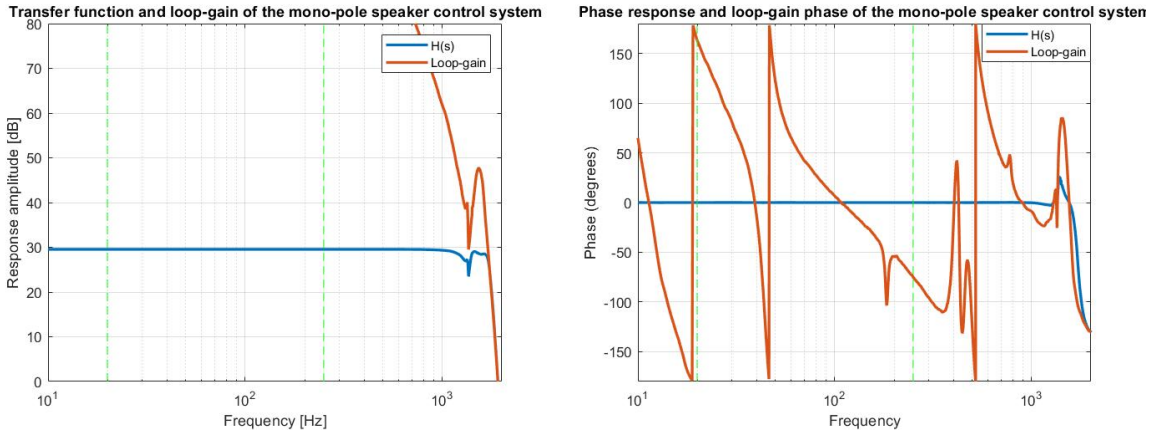

(a) The frequency response of the system.

(b) The phase response of the system.

Figure 5.24: The system response after adding a simple high-pass filter, a high order low-pass filter and the inverse of the model of the speaker to the controller

5.5.4. Controller choice

Now that the three potential controllers have been discussed, it is time to decide on what controller will be used based on the pros and cons of all three controllers.

PD controller

The PD controller shows very promising results. The pass-band is relatively flat for both the frequency and the phase response. It should also be easily implementable in the digital chip since it only consists of a derivative controller. A downside of the derivative controller is that the loop-gain for frequencies below the pass-band is low resulting in poor performance of the system at these frequencies.

Adding frequency specific gain

Adding specific gain at specific frequencies yields an unstable system leading to little extra loop-gain. Due to this lack of loop-gain, the frequency response is not flat inside the pass-band. The design could be optimized to improve the loop-gain but this would come at the cost of even more fluctuation in the phase response, eventually leading to instability. It is, however, fairly easy to implement the controller and may thus still prove useful, even when the digital signal processing unit has very limited possibilities.

Constant loop-gain

Making the loop-gain constant inside the pass-band by using the inverse of the model of the speaker, results in a flat frequency and phase response. Performance outside the pass-band is also as required and the system is very stable. A downside of this controller is that it may be difficult to implement it digitally since a precise frequency response is required.

From the three controller options mentioned, the constant loop-gain controller will be chosen. The reason for this is that the response in the pass-band is the flattest compared to the other two implementations. A possible downside to choosing this controller is that it is hard to implement and the ADAU chip may thus not be able to handle this controller.

Even though the controller is now designed, there are still some negative effects coming from the ADAU that influence the performance of the system. First of all, the delay caused by the ADAU1777 chip will be discussed. Secondly, the quantization noise caused by the ADC will be discussed and modelled.

5.5.5. Delay

The delay caused by the ADAU1777 chip is the major reason why the ADAU1777 chip is used for this implementation, this is because it is very low compared to other acoustic processing devices. Depending on the

sampling frequency chosen, the ADAU will have a certain latency. According to the datasheet [4], the latency at a sampling frequency of $192kHz$ should be approximately $38\mu s$ and at a sampling frequency of $768kHz$ this delay would decrease to $10\mu s$. These delays are low when compared to the delay caused by the speaker, especially when taking into account that this device can perform a small but sufficient selection of signal processing. The effect of this delay on the stability of the system will thus also be little. The difference in effect on the system between these two sampling frequencies is small and both will thus do a sufficient job. Due to this, choosing the ADAU1772 [3], could also be used to implement the controller. The low latency in these two chips comes however with a cost. Even though these systems can do some decent but simple signal processing, they are limited especially when compared to other devices provided by the same manufacturer. Some of the controllers that were designed require some specific signal processing and the question is whether or not this is possible in the previously mentioned chips. Since a physical implementation of the system will not be made, this will not be further researched but it is definitely something to take into account while actually building a control system using this chip.

5.5.6. ADAU noise

The ADAU1777 is a coder-decoder (codec) that possesses 24-bit sigma-delta analog-to-digital (ADC) and digital-to-analog (DAC) converters[4]. A noise analysis will be made for this component. In addition, a noise model will be made to determine the influence of the analysed noise on the system.

Two main noise sources are inherent to sigma-delta converters, namely:

- Quantization noise
- Thermal noise

Quantization noise is a limiting factor for an ADC's dynamic range [12]. Quantization noise results from the conversion of a continuous random variable to a discrete random variable [8]. Similarly, quantization noise can also arise when a discrete random variable is converted to a discrete random variable with fewer levels [8]. The quantization error can be modelled as random or white noise under the assumption that the quantization error is random as well [12]. The probability density function (PDF) of this quantization noise is shown in Figure 5.25.

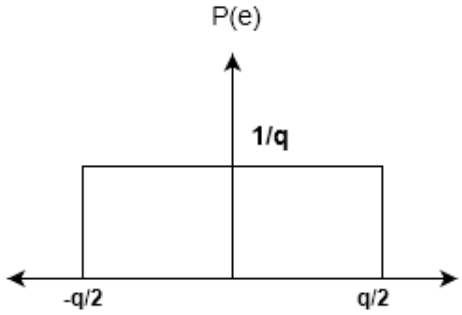

Figure 5.25: The probability density function of the quantization error. Here q denotes the lsb (equivalent to Δ used in the rest of the report)

The quantization noise power can be found by means of Equations (5.11) and (5.12) respectively.

$$e(t) = st \qquad for \quad \frac{-\Delta}{2s} < t < \frac{\Delta}{2s} \tag{5.11}$$

$$\overline{e^2(t)} = \frac{s}{\Delta}\int_{\frac{-\Delta}{2s}}^{\frac{\Delta}{2s}} (st)^2 dt = \frac{\Delta^2}{12} \tag{5.12}$$

The quantization voltage is given by Equation (5.13)

$$\sqrt{\overline{e^2(t)}} = \frac{\Delta}{\sqrt{12}} \tag{5.13}$$

As mentioned before the ADCs and DACs are sigma-delta modulators. These modulators have certain properties that differ from Nyquist based modulators, namely:

- Oversampling
- Noise shaping

Oversampling essentially means that the input signal is sampled at a frequency much larger than the Nyquist frequency ($F_s \gg 2 \times B$, with B being the input bandwidth). One advantage of oversampling is that the quantization noise in the band of interest is reduced [12].
Noise shaping filters in sigma-delta converters ensure that the quantization error or quantization noise is distributed in such a way that it is minimal in the frequency band of interest [12]. These two concepts are important to consider when modelling the noise of a sigma-delta modulator. The SNR is of importance as well. The SNR for a sigma-delta converter is given by Equation (5.14) [12]. Here b is the number of bits, F_s is the sampling frequency and F_0 is the frequency band of interest.

$$SNR = 1.76 + 6.0206b + 10log_{10}(\frac{Fs}{2 \times F_0}) \tag{5.14}$$

The theoretical SNR is calculated by means of Equation (5.14) and this is found to be $163dB$ (with $b = 24$, $F_s = 96kHz$ and $F_0 = 1kHz$). However the practical SNR has a value of $102dB$ for a bandwidth of $20kHz$ [4], therefore the number of effective bits can be calculated by means of Equation (5.14) (with $SNR = 102dB$, $Fs = 96kHz$ and $F_0 = 20kHz$). This results in the number of effective bits being 16. A new practical SNR estimate can be made assuming that the bandwidth of interest is 1 kHz. Applying the previously calculated number of effective bits (16 bits) to Equation (5.14), results in a practical SNR of 115 dB (with $Fs = 96kHz$ and $F_0 = 1kHz$).

ADAU noise model
As previously discussed the effective number of bits is 16 which is much lower than 24 bits. The error related to this number of bits can be calculated by means of Equations (5.15) and (5.16) respectively. The numerator of Equation (5.15) corresponds to the input voltage range of the ADAU.

$$\Delta = \frac{3.3}{2^{16}} \approx 50.35\mu V \tag{5.15}$$

$$e = \frac{\Delta}{\sqrt{12}} \approx 14.54\mu V \tag{5.16}$$

To make a noise model, the in band quantization noise power will be used and this is given by Equation (5.17). Here, F_0 denotes the input signal bandwidth and F_s denotes the sampling frequency [12]. This equation is obtained by squaring the noise power spectral density and integrating it over the bandwidth of interest (1 kHz). The derivation and procedure of this process can be found in Appendix D.

$$n_o = e\frac{\pi}{\sqrt{3}}(\frac{2F_0}{F_s})^{\frac{3}{2}}(V) \tag{5.17}$$

A data-set has been made with randomized error values chosen between $-e/2$ and $e/2$, where e is the value given in Equation (5.16). The power spectral density is determined for this data-set and the result can be seen in Figure 5.26a. The quantization noise power is shown in Figure 5.26b, here the red line signifies the average of the quantization noise power and this has been obtained by means of a moving average filter.

This noise model N_A will be used in the transfer function $S_A(s)$ which represents the propagation of N_A through the system. The transfer function is given by Equation (4.8) and the result of the added noise source N_A on the system is shown in Figure 5.27.

5.5.7. Conclusion

The controller is designed and the negative effects coming from the digital implementation have been discussed. The filters used to suppress unwanted frequencies are designed to be a low- and high-pass cutt-off filters. These filters do however cause phase fluctuations in the loop-gain and this could have a negative effect on the stability of the system. Another major downside to these filters is that they should be placed and designed very carefully to make sure they do not have a negative influence on the stability and performance of the system. A small fluctuation in the cut-off frequency or order of the filter can lead to great problems occurring in the system. The controller was chosen to be the inverse of the model of the speaker. By using this controller, the loop-gain will become nearly constant inside of the pass-band and will thus maximally

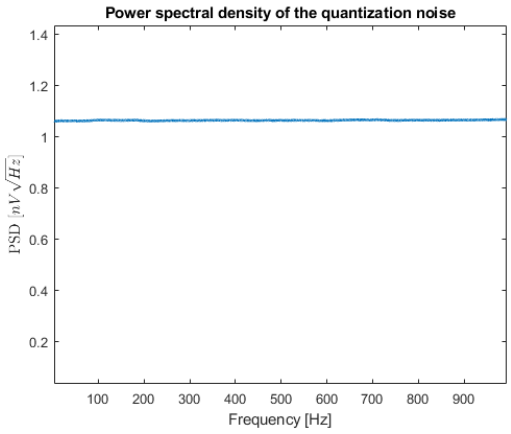

(a) The power spectral density of the noise data given in $\frac{nV}{\sqrt{Hz}}$.

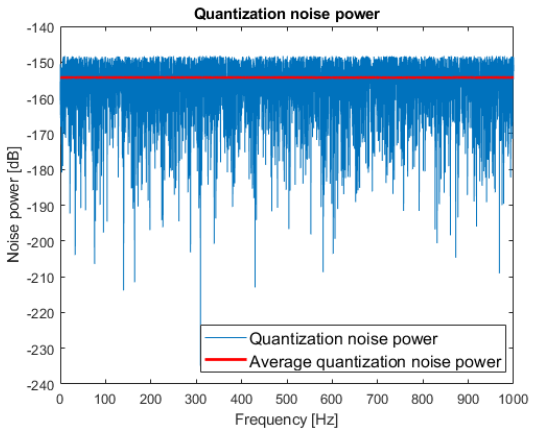

(b) Quantization noise power of sigma delta modulators given in dB.

Figure 5.26: Initial system response without any signal processing done in the controller.

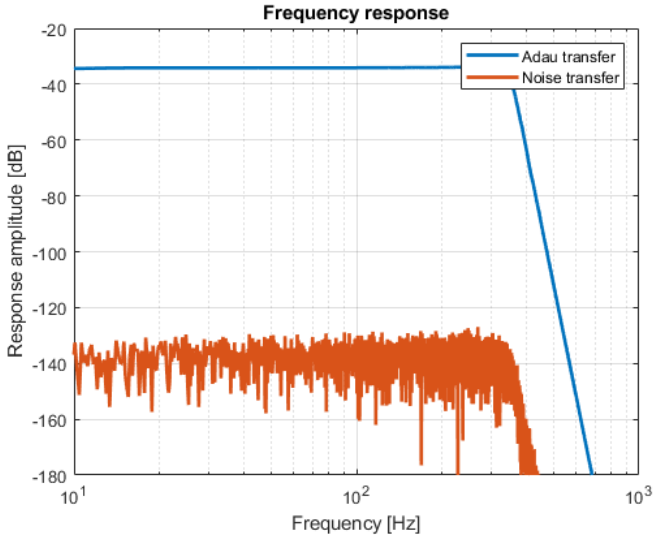

Figure 5.27: Frequency response of the transfer function from Equation (4.8) and when ADAU noise is added to the system.

utilize the loop-gain. A downside to this controller is that it might be too complex to be implemented by the ADAU. The delay of the ADAU chip will not cause major problems since the maximum delay will be $38\mu s$, which is less than the delay induced by the speaker. It will however add to the total system delay. Later on, a delay analyses will be given that takes all the delays of the system into account.

5.6. Voltage amplifier

In the designed circuit shown in Figure 4.6, the voltage amplifier (M) is present. This component refers to a voltage amplifier that amplifies the error signal e (Figure 4.6) in the analogue domain. Section 5.6.1 will describe what the relevance is of the error signal (e). It shows that an amplification of the error signal e is desired to minimize the influence of quantization noise and quantization errors. The expected result of an amplification of the error signal e is that the ADC from the ADAU will use more bits effectively and the error signal e is better represented. An added advantage is that extra loop-gain is already added due to this amplification.

5.6.1. Error signal relevance

The ADAU consists of 24 bit ADC´s and DAC´s, since the maximum input and output voltage is $3.3V_{pp}$, the LSB represents approximately $200nV$ as is shown in Equation (5.18) [20]. This also means that the different

levels of the digitization have a gap of $200nV$ between them. In Equation (5.15) it is shown that the sensitivity is approximately $50.35\mu V$ when the ADC only has the resolution of 16 bits that is derived in Section 5.5.6.1.

$$V = \frac{3.3}{2^{24}} = 1.97 * 10^{-7} \approx 200nV \tag{5.18}$$

The question now is whether or not this precision is enough to produce clear audio even for very low audio levels. For the minimum audio volume produced by the speaker, $10dB_{SPL}$ is chosen, this is equivalent to the sound of light leaf rustling and calm breathing [27]. To check what voltage level at the speaker input is required to produce this sound volume, the data sheet of the speakers is used [16]. This data sheet indicates that the speaker produces around $90dB_{SPL}$ at speaker input voltage of 2.83V, at a measurement distance of 1 meter. To determine what speaker input voltage is related to $10dB_{SPL}$, the following calculations were used:

$$\frac{90dB_{SPL}}{10dB_{SPL}} = \frac{10^{\frac{90}{20}}}{10^{\frac{10}{20}}} \frac{31.6 * 10^4}{3.16} = 10^4 \tag{5.19}$$

Scaling the required speaker input voltage to this relative difference given in Equation (5.19) gives:

$$\frac{2.83}{10^4} = 0.283mV \tag{5.20}$$

The outcome of Equation (5.20) is the required voltage at the speaker to produce the minimum noticeable sound, which was previously determined to lay at $10dB_{SPL}$. The system (as given in Figure 4.5) adds a gain of 30 from input to output in the pass band which means that the input voltage of the system corresponding to $0.3mV$ at the input of the speaker is equal to the following:

$$\frac{0.283mV}{30} = 9.43\mu V \tag{5.21}$$

Using the outcome of Equation (5.21) it is possible to predict in what order the error signal will be. By taking sinusoids with an amplitude of $10\mu V$ and frequencies varying between the frequencies in the pass-band as an input to the system, it is possible to find out what the amplitude of the error signal e will be for different sinusoidal inputs. For some frequencies, the error signal can be somewhere in the order of $10nV$. The LSB of the ADC represents $200nV$ meaning that it will not capture voltages in the order of $10nV$ and these error signals will thus not be represented. The quality of the audio will thus drastically decrease, especially at lower volumes. It must be noted that the resolution from the ADAU is given as 24 bits, but the practical resolution may be lower meaning that the gap between each digitization level may be larger than $200nV$.

5.6.2. Pre-ADAU-amplifier M

As given in the previous section, the error signal can be as small as $10nV$ and still cause audible output voltages as described in the section above. By amplifying this error signal significantly, the relevant signals can be digitized by the ADC and more of the ADC's resolution can be used. An analogue amplifier in front of the ADC can accomplish this result. The amplification can be done either using the gain from the subtraction circuit or by adding another amplifier. Adding loop-gain can be done in a number of components, of which the voltage amplifier is one. But the voltage amplifier should not handle all the loop-gain. This is due to the input and output voltage limitations from the ADAU1777. These limitations are presented in Table 5.2 for the monopole speaker and in Table F.1 for the dipole speaker.

Subtraction circuit

One method for amplifying the voltage of the error signal is by making use of the subtraction circuit as given in Section 5.2.2.2. The gain is set as defined by Equation (5.2).

Custom amplifier

Another option is to insert an amplifier between the adder and ADC from the ADAU1777. A simple voltage amplifier is given in Figure 5.28. Assume a voltage amplification A_d is needed, then Equation (5.22) gives the ratio between the two resistors given in this voltage amplifier circuit.

$$\frac{R_2}{R_1} = A_d - 1 \tag{5.22}$$

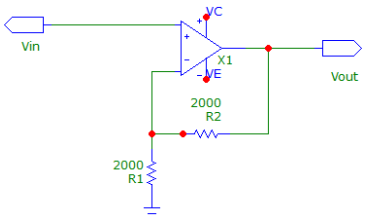

Figure 5.28: Voltage amplifier for component M, the voltage amplifier

Conclusion for pre-ADAU-amplifier M
Making use of the already in place subtraction circuit seems the best solution as this circuit will increase CMRR and SNR when gain is added in this circuit. Besides, adding another voltage amplifier in the system as is suggested with the custom amplifier only increases the noise entering the ADC. By choosing the subtraction circuit to be the amplifier, no extra delay will be added in addition to the delay given by this circuit and a delay that is already present is small enough to neglect.

5.7. Total system

Now that all individual components are designed, it is time to analyse the system as a whole. The stability and the corresponding Nyquist plot can be determined. Besides this, the maximum voltages that the components can encounter will be derived and the effect of the delay of the components can also be determined. In this section it is still assumed that no noise or non-idealities are present in the system and thus the system schematic that is given in Figure 4.6 will be used. How these noise sources will influence the system and how the system should be adjusted to handle this will be discussed in Section 5.8.

5.7.1. Stability

The designed system would be useless if it was unstable and a stability analysis should thus be done to check whether or not the system can handle the loop-gain in the system. The chosen system is the one corresponding to the constant loop-gain controller given in figure 5.24. The Nyquist plot of the system will be used to check the stability and it is given in Figure 5.29b. Similar plots for the dipole can be found in Figure F.1 (response after added gain). For this configuration of the monopole speaker control system, the Gain Margin is $2.4 * 10^{3}$° and the Phase Margin is 106°.

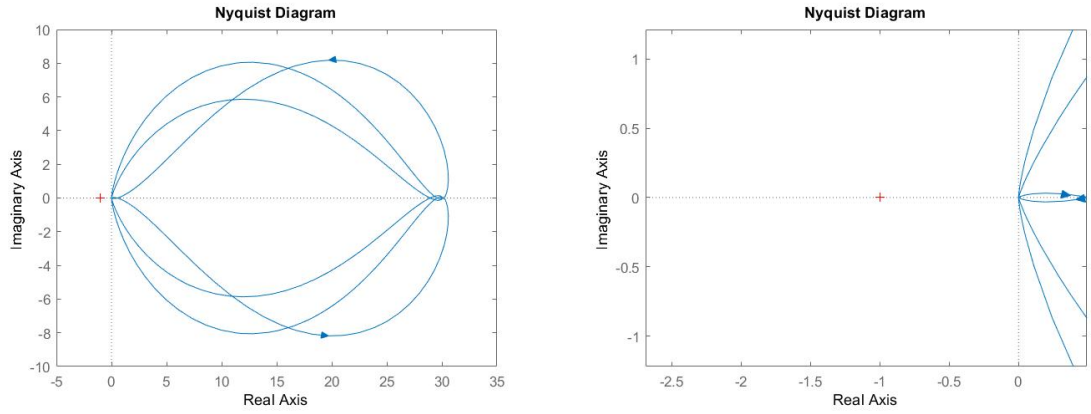

(a) The Nyquist plot before adding additional gain

(b) The Nyquist plot after adding additional gain

Figure 5.29: The Nyquist plots showing the stability of the system before and after additional loop-gain is added.

5.7.2. Maximum system voltage

Now that the design for the components is determined it should still be checked whether or not the system components can handle the voltages which are present at their in and output. To be able to check this, the output voltage of every component will be checked for all frequencies inside the pass-band. In other words,

for every component in the system, the maximum output voltage will be determined by checking the component's output voltage when a sinus with frequencies varying over the entire pass-band and with an amplitude of $1V$ will be delivered to the input of the system. The result of this computation can be found in Table 5.2. All these maximum voltages are achievable by the components and thus the component limitations will not

Component	Maximum output voltage
Adder	$354\mu V_p$
Voltage amplifier	$1.1V_p$
ADAU 1777 chip	$2.1V_p$
Voltage to current amplifier	$63V_p$
monopole Speaker	$30.1V_p$
System gain	$1.0036V_p$

Table 5.2: The maximum output voltage found for each component in the monopole speaker control system for an input sinusoid of amplitude $1V$.

be a problem. A similar table for the dipole speaker can be found in Table F.1, for the dipole speaker control system there are also no problems regarding output voltages.

5.7.3. Delay in the system

In the previous sections, the delay caused by the components was derived. There are three components which do not have a negligible delay and these will be considered while deriving the delay in the system. To recap, the delays in question are the monopole speaker delay of $210\mu s$ ($160\mu s$ for the dipole speaker), the ADAU latency of $10\mu s$ and the voltage to current amplifier with a delay of $30\mu s$. These delays can be used to derive the time delays and thus also the maximum phase delay in the pass-band. The high cut-off frequency of the control system of the monopole speaker is equal to 250 Hz and the phase delay at this frequency is found to be [10]:

$$\angle o = -\omega * T_D = 2 * \pi * f * T_D = 2 * \pi * 250 * (10\mu s + 30\mu s + 210\mu s) = 0.39rad = 22.5° \tag{5.23}$$

The same can be done for the dipole speaker, for which the high cut-off frequency of the control system is 800 Hz. The corresponding phase delay is found to be:

$$\angle o = -\omega * T_D = 2 * \pi * f * T_D = 2 * \pi * 800 * (10\mu s + 30\mu s + 160\mu s) = 1.0rad = 57.6° \tag{5.24}$$

These phase shifts are not at all endangering the stability of the system since they are far less than a phase delay of 180° that is required to make the system unstable.

5.8. Noise in the system

As mentioned before, the total noise in the system comprises of three main noise sources namely:

- N_A representing the quantization noise in the ADAU.
- N_K representing the voltage to current amplifier noise. The characteristics of this noise are provided by the amplifier subgroup.
- N_M represents the noise generated by the accelerometer.
- N_L represents the distortions from the loudspeaker which is modelled as noise.

Each of these noise sources has been discussed in their respective parts and models have been made. The effect of the noise sources on the total system are investigated and the result of the monopole speaker is shown in Figure 5.30. From this figure it can be concluded that the accelerometer/distortion noise is suppressed by 30 dB, the ADAU noise is suppressed by 70 dB, the amplifier noise is suppressed by approximately 80-100 dB and the loudspeaker distortions are suppressed by approximately 100 dB.

Even though the noise sources are suppressed, they can still influence the performance of the system. The noise will not only influence how the user will perceive the music, but it can also lead to instability in the system. Due to the suppression of the noise sources, its influence on the stability is very limited and only

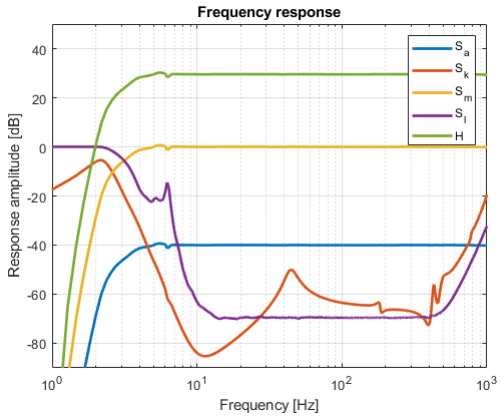

Figure 5.30: The transfer function H and the transfers of the three main noise sources.

a very minor decrease in loop-gain might be necessary to make sure the system will not become unstable. The Nyquist plot of the system with and without the noise sources, implemented as modelled in the previous sections, is shown in Figure 5.31 for the monopole filter. A similar plot for the dipole filter can be found in Figure G.1. In the Nyquist plot it can be seen that adding noise to the system does not affect the stability of the system drastically. The plot does not encircle the -1 point, indicating that the system is stable. Besides this, the GM and PM do not change (noticeably) after adding the noise to the system. The margins indicate that the loop-gain could be even further increased, this is not done however due to the reasons mentioned in the following subsection.

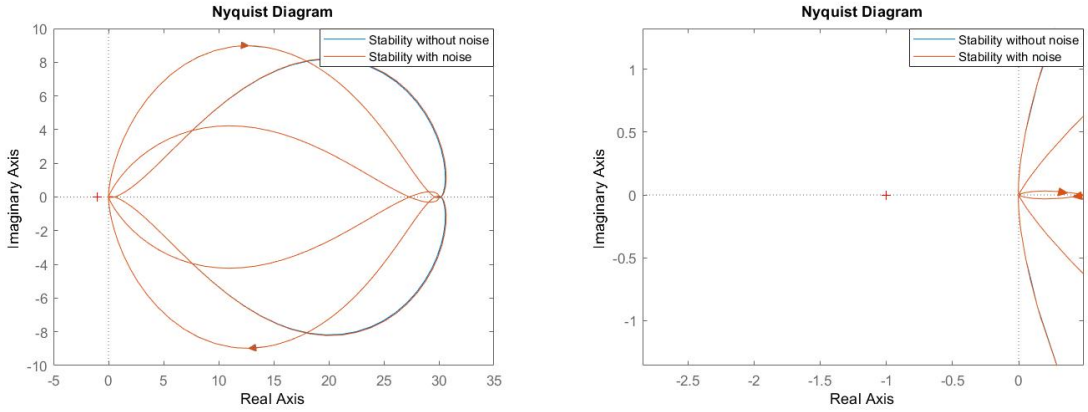

(a) The Nyquist plot with and without added noise to the system

(b) The Nyquist plot zoomed in to the -1 point

Figure 5.31: The Nyquist plot of the control system surrounding the mono-pole speaker with and without added noise sources

5.8.1. Discussion on the noise

Even though the Nyquist plots, shown in Figure 5.31, show that the noise has very little influence on the system, this doesn't represent reality. The reason for this is that one very important and unrealistic assumption was made during the determination of the influence of noise on the system. This assumption is that the noise is represented by their respective models and that these models are time-invariant. By making this assumption, the control system can maximally suppress the noise in the system. When fluctuations in the noise start to appear, the error caused by these fluctuations will increase and this will have a more severe influence on the system's stability. To what extent this will influence the system performance is unknown and will not be further examined due to time and complexity reasons. The loop-gain will also not be adjusted and will remain as is.

6
Discussion

This thesis is fully based on theoretical research and thus the main point up for discussion is the practical implementation. Even when simulations show the expected outcome, real-life tests should be done to make conclusions regarding a practical implementation. This does not take away however that some theoretical statements made in this thesis are up for discussion.

For this project, it is a given that the sensor at hand will be an accelerometer placed on the cone of the speaker. Noise from this source is already limited and acceleration as feedback is optimal because the cone's acceleration is directly proportional to the current driving the speaker. Alternative sensors may, however, offer less noise and result in less error to suppress and /or have higher accuracy. The same reasoning can be applied to the digital processing chip, the ADAU1777. A similar chip, the ADAU1772, has also been investigated but emphasise was put on the ADAU1777 as a given of the project. During the project, it was constantly assumed that the accelerometer provides unity gain on the acceleration to voltage transition. In fact, this is not the case and some scalar should be implemented to achieve the unity gain for this component. Besides this, the frequency response of the accelerometer in the pass-band of interest is not entirely flat, as is assumed.

The designed controller uses the inverse of the model of the speaker. This means that not only the real part but also the complex part will be inverted. Whether or not this will lead to a non-causal system is not investigated. If it is non-causal, the controller will add an extra time delay to the system.

Analogue components have been used in the design. Their types and values have not specifically been suggested for a true final design. The currently used components have been used for verification of the designs. The opamp used is the OPA177 [25], which is a high-precision opamp, but the input noise voltage is rather large ($85\frac{nV}{\sqrt{Hz}}$). This leads to noise issues on the alternative circuit that is discussed. Although the noise would still be significantly large, opamps with lower input noise voltage would increase the SNR of the alternative opamp circuit. The full impact of noise on the full system, that the suggested instrumentation amplifier circuit introduces, is not simulated or measured. The noise it does produce has only been simulated and measurements on a physically built system would have to show whether the noise it produces truly is or isn't significant.

The influence of the noise on the stability of the control system is yet to be analysed. Even though it is found that the defined noise sources are suppressed in the system, the actual influence and behaviour of noise varying in time is yet to be determined.

7

Conclusions, recommendations and future work

The main scope of this thesis is about the digital implementation of motional feedback in a bass loudspeaker. This thesis succeeded in providing methods on how to accomplish the digital implementation and it shows several factors to take into account and what alternatives are present. Moreover, this thesis also substantiates the choice for several design alternatives.

The accelerometer is the first component that makes a feedback-loop possible. Although some good alternatives, such as a microphone or light-based-sensors, have been discussed, it does make perfect sense to use an accelerometer due to the acceleration being directly proportional to the current that is driving the speaker. The accelerometer noise has been modelled based on the mechanism of Brownian Motion. It was also found that $1/f$ noise dominates at low frequencies, therefore the decision has been made to make a combination noise model. This combination noise model consists of Gaussian white noise for low frequencies and Brownian noise for higher frequencies (20-300 Hz).

By introducing a feedback loop, the system will be pushed to a $0dB$ gain when an amplification of $\frac{1}{30}$, 30 being the desired gain, is not provided in the feedback loop. According to the requirements, a gain of $30 = 29.54dB$ is desired. A simple voltage divider can be set in place to achieve this result.

From comparisons on noise and CMRR it can be concluded that an instrumentation amplifier circuit is the optimal circuit to subtract the feedback signal from the input signal. It directly offers a very low load to the voltage divider and can also function as an amplifier. This is beneficial because the small error signal is then increased significantly before the ADAU's ADC will transform a continuous-time signal into a discrete-time signal. The amplification provided by this circuit contributes to loop-gain and increases the SNR of the instrumentation amplifier circuit up to $118.7dB$. The distortion that occurs at this point, despite the large SNR, can be suppressed as well. Quantization noise was found to be the most prominent noise source concering the ADAU. 16 effective bits are used in the sigma delta modulators of the ADAU, resulting in a SNR of 115 dB for a bandwidth of 1 kHz. The noise model has been obtained by calculating the in band quantization noise power for a randomized dataset.

The loop-gain in the system is large enough to not only add input to output gain to the system but also increase flatness inside the pass-band. Due to the controllers, the system is made stable and thus capable to handle more loop-gain than was possible before a controller was implemented. The filters in the controller make sure that unstable frequencies outside of the pass-band are suppressed such that they do not make the system unstable.

The feedback loop and the control system are put in place in order to control a speaker which is driven by a voltage to current amplifier. What this amplifier does in the system is adding loop-gain. Moreover, the amplifier has been designed in another project with keeping in mind a THD limit of only 0.001%. Still, the noise that might be introduced by this amplifier is suppressed. The amplifier noise model has been obtained by means of the data provided by the amplifier subgroup.

All the components in the feedback loop can handle the voltages which may be present at their in- and outputs. The most important limitation are the in and output voltage of the ADAU and these are not surpassed with the current system implementation. Further increasing the loop-gain in the system will only alter this if the noise signals will become present drastically due to large amplification.

The delay induced by the components was found to be small enough to not make the system unstable. A phase shift of 180° would lead to an unstable system but the delay will maximally be 57.6° which will thus not lead to problems.
All the modelled noise sources will be suppressed by the system. The non-linearities originating from the speaker and the noise coming from the accelerometer will be suppressed with $29.54dB$. The noise coming from the voltage to current amplifier will be greatly suppressed with $70dB$. Finally, the quantization noise originating from the ADC of the ADAU will be suppressed with $80-100dB$.

Appendices

A

Transfer functions derivation

A.1. Modelling the motion feedback system

The entire system can be modelled as given in figure A.1 The function describing the output Y can be derived as follows:

$$f = (Y(s) + N_m) * P \tag{A.1}$$

$$e = i - f = X(s) - (Y(s) + N_m) * P \tag{A.2}$$

$$Y(s) = ((e * M + N_a) * D(s) * K + N_k) * G(s) = (((X(s) - (Y(s) + N_m) * P) * M + N_a) * D(s) * K + N_k) * G(s) \tag{A.3}$$

$$Y = ((X(s) * M - Y(s) * P * M - N_m * P * M + N_a) * D(s) * K + N_k) * G(s) \tag{A.4}$$

$$Y = (X(s) * M * D(s) * K - Y(s) * P * M * D(s) * K - N_m * P * M * D(s) * K + N_a * D(s) * K + N_k) * G(s) \tag{A.5}$$

$$Y = X(s)*M*D(s)*K*G(s) - Y(s)*P*M*D(s)*K*G(s) - N_m*P*M*D(s)*K*G(s) + N_a*D(s)*K*G(s) + N_k*G(s) \tag{A.6}$$

$$Y(1+P*M*D(s)*K*G(s)) = X(s)*M*D(s)*K*G(s) - N_m*P*M*D(s)*K*G(s) + N_a*D(s)*K*G(s) + N_k*G(s) \tag{A.7}$$

$$Y = \frac{X(s) * M * D(s) * K * G(s) - N_m * P * M * D(s) * K * G(s) + N_a * D(s) * K * G(s) + N_k * G(s)}{1 + P * M * D(s) * K * G(s)} \tag{A.8}$$

This equation can be subdivided to show the transfer function belonging to the different sources:

$$Y = H * X + S_a * N_a + S_k * N_k - S_m * N_m \tag{A.9}$$

Where the transfer function per source is given as:

$$H(s) = \frac{M * D(s) * K * G(s)}{1 + M * D(s) * P * K * G(s)}, \text{transfer function of the source signal} \tag{A.10}$$

$$S_A(s) = \frac{D(s) * K * G(s)}{1 + M * D(s) * P * K * G(s)}, \text{transfer function of ADAU noise} \tag{A.11}$$

$$S_K(s) = \frac{G(s)}{1 + M * D(s) * P * K * G(s)}, \text{transfer function of amplifier output noise} \tag{A.12}$$

$$S_M(s) = \frac{P * M * D(s) * K * G(s)}{1 + M * D(s) * P * K * G(s)}, \text{transfer function of accelerometer noise} \tag{A.13}$$

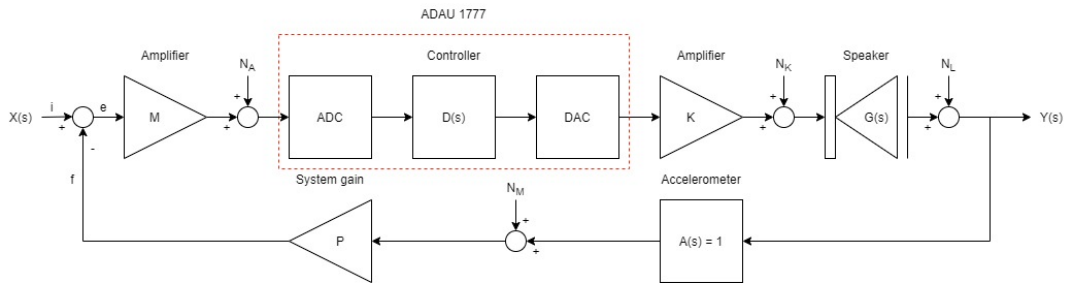

[H]

Figure A.1: The schematic describing the control system.

B

Adder - Subtraction circuit

B.1. Equations

In chapter 5.2.2, multiple designs are given as design for the adder. The adder is the component in the system that subtracts the feedback signal from the input signal. For two of the three given designs (the instrumentation differential amplifier circuit and the alternative non-differential circuit), noise equations due to noise have been composed. These equations have been composed using SLiCAP [17]. The approximated equations are given in the report itself (Equations 5.4 and 5.4). These equations have been derived from Equations B.1 and B.2. In these equations, S is the output noise power given in $\frac{V^2}{Hz}$, S_i is the amplifier input noise current given in $\frac{A^2}{Hz}$ and S_v is the amplifier input noise voltage given in $\frac{V^2}{Hz}$. The resistor values have reference to the resistors given in Figures 5.6b and 5.6c with respect to the given Equations B.1 and B.2.

$$
\begin{aligned}
S = {} & \frac{S_{v3}(R_5+R_6)^2)}{R_5} + 4kTR_6 + \frac{R_3^2R_6^2S_{i2}}{R_5^2} + \frac{S_{i3}(R_4R_5R_6+R_4R_5R_7+R_4R_6R_7+R_5R_6R_7)^2}{R_5^2(R_4+R_7)^2} + \frac{4kTR_6^2}{R_5} \\
& + \frac{4kTR_3R_6^2}{R_5^2} + \frac{S_{v2}(R_1R_4R_6+R_3R_4R_6+R_1R_6R_7+R_2R_5R_7+R_2R_6R_7+R_3R_6R_7)^2}{R_1^2R_5^2(R_4+R_7)^2} \\
& + \frac{S_{v2}(R_1R_5R_6+R_3R_4R_6+R_1R_6R_7+R_2R_5R_7+R_2R_6R_7+R_3R_6R_7)^2}{R_1^2R_5^2(R_4+R_7)^2} + \frac{4kT(R_3R_4R_6+R_2R_5R_7+R_2R_6R_7+R_3R_6R_7)^2}{R_1R_5^2(R_4+R_7)^2} \\
& + \frac{R_2^2R_7^2S_{i1}(R_5+R_6)^2}{R_5^2(R_4+R_7)^2} + \frac{4kTR_2R_7^2(R_5+R_6)^2}{R_5^2(R_4+R_7)^2} + \frac{4kTR_4R_7^2(R_5+R_6)^2}{R_5^2(R_4+R_7)^2} + \frac{4kTR_4^2R_7(R_5+R_6)^2}{R_5^2(R_4+R_7)^2}
\end{aligned}
\tag{B.1}
$$

$$
\begin{aligned}
S = {} & R_{10}^2S_{i2} + 4kTR_{10} + S_{v2}\frac{(R_{13}R_8+R_{13}R_{10}+R_8R_{10})^2}{R_{13}^2R_8^2} + S_{i1}\frac{R_{12}^2R_{10}^2}{R_{13}^2} + 4kT\frac{R_5^2}{R_3} + 4kT\frac{R_5^2}{R_4} \\
& + S_{v1}\frac{R_{10}^2(R_{11}+R_{12})^2}{R_{11}^2R_{13}^2} + 4kT\frac{R_{12}R_{10}^2}{R_{13}^2} + 4kT\frac{R_{12}^2R_{10}^2}{R_{11}R_{13}^2}
\end{aligned}
\tag{B.2}
$$

B.2. Figures

The instrumentation differential amplifier should have no increased common-mode gain when the circuit gain is increased. The same goes for the noise. Proof is given by Figures B.1 and B.2. These figures relate to Figures 5.11 and 5.12 (the circuits without gain) respectively.

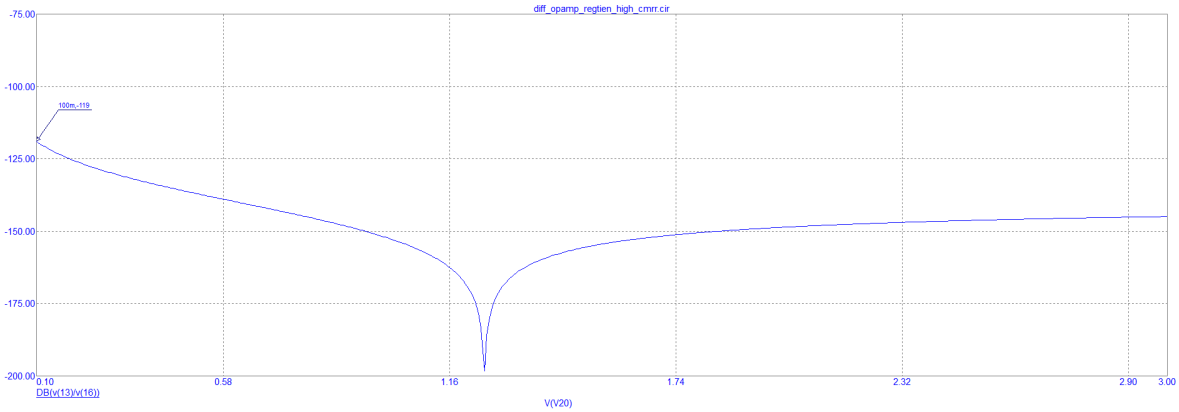

Figure B.1: Common mode gain behaviour of the instr. differential amplifier with a gain of 30. $V(V20) = V(16) = V_{cm}, V(13) = V_{out}$

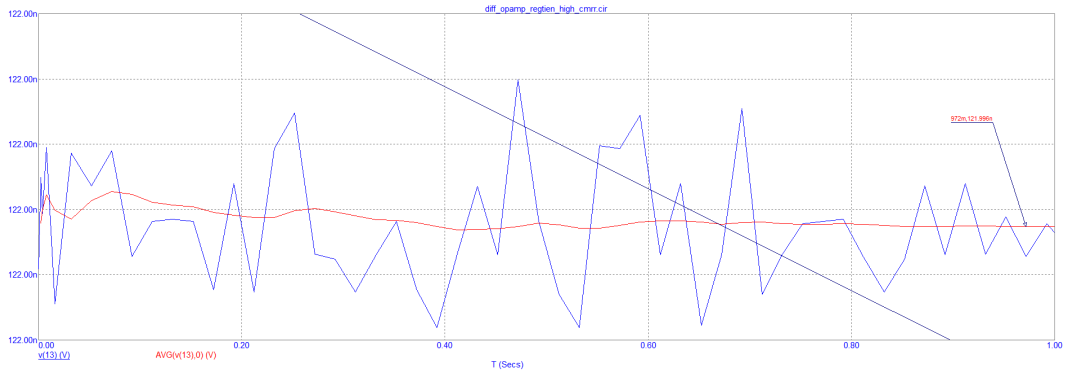

Figure B.2: Output noise of the instr. differential opamp circuit with a gain of 30, averaged over time. $V(13) = V_{out}$

C
Speaker

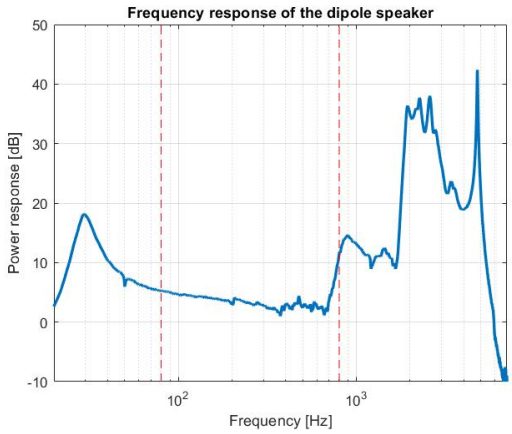

(a) The frequency response of the speaker.

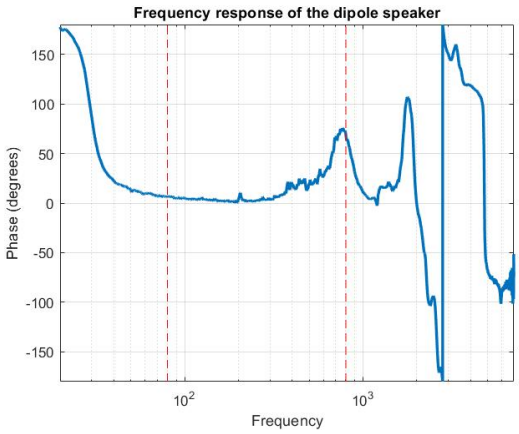

(b) The phase response of the speaker.

Figure C.1: Frequency and phase response of the dipole speaker. The red lines indicate the minimum pass-band which should be controlled and receive the specified gain.

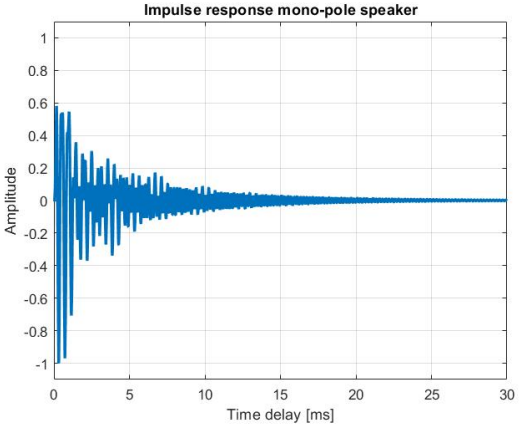

(a) Impulse response of the speaker.

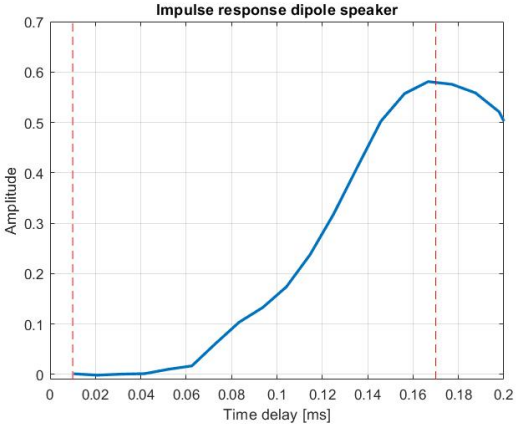

(b) Zoomed in impulse response to determine the delay of the system.

Figure C.2: Impulse response of the dipole speaker used to determine the delay it inflicts on the system. The red lines indicate the time instance which is considered to represent the delay of the speaker.

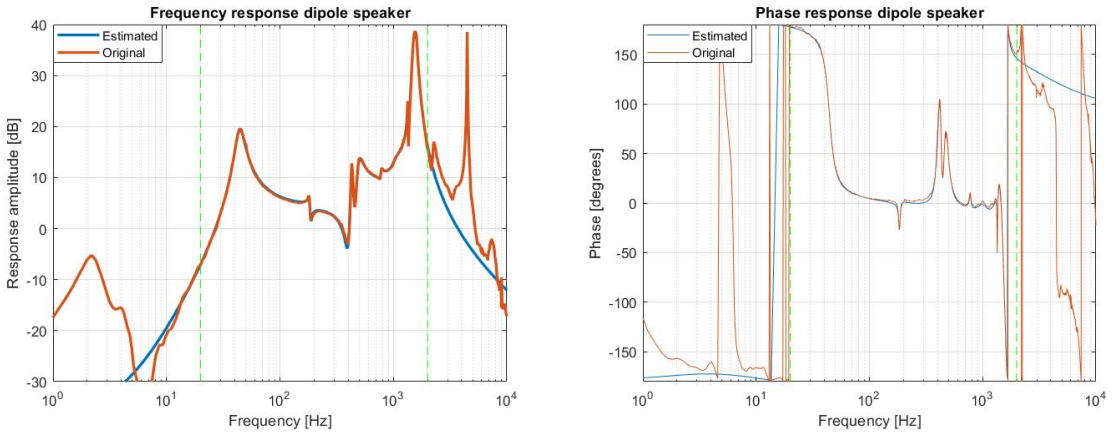

(a) The actual and the model of the dipole frequency response.

(b) The actual and the model of the dipole phase response.

Figure C.3: Modelling the dipole speaker into a transfer function. The frequency range indicated by the green dotted lines indicate the range for which the speaker was modelled.

D

Quantization noise

Noise spectral density in a Nyquist based ADC. Where all noise power is folded into the frequency band of $0 \leq F \leq \frac{F_s}{2}$

$$E(f) = e(\frac{2}{F_s})^{\frac{1}{2}} \quad (\frac{V}{\sqrt{Hz}}) \tag{D.1}$$

In band quantization noise power:

$$n_0^2 = e^2(\frac{2F_0}{Fs}) \quad (V^2) \tag{D.2}$$

$$n_0 = e(\frac{2F_0}{Fs})^{\frac{1}{2}} \quad (V) \tag{D.3}$$

Sigma delta modulator noise:

$$n_i = (e_i - e_{i-1}) \tag{D.4}$$

Noise spectral density in a sigma delta modulator using the previously determined noise spectral density $E(f)$:

$$N(f) = E(f)|1 - e^(\frac{-j\omega}{F_s})| = 2e(\frac{2}{F_s})^{\frac{1}{2}} sin(\frac{\omega}{2F_s}) \quad (\frac{V}{\sqrt{Hz}}) \tag{D.5}$$

In band quantization noise power in a sigma delta modulator:

$$n_0^2 = e^2(\frac{\pi^2}{3})(\frac{2F_0}{Fs})^3 \quad (V^2) \tag{D.6}$$

$$n_0 = e(\frac{\pi}{\sqrt{3}})(\frac{2F_0}{Fs})^{\frac{3}{2}} \quad (V) \tag{D.7}$$

E

Controller

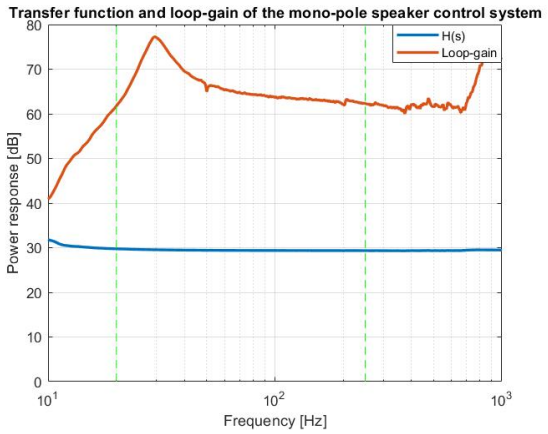

(a) The frequency response of the system.

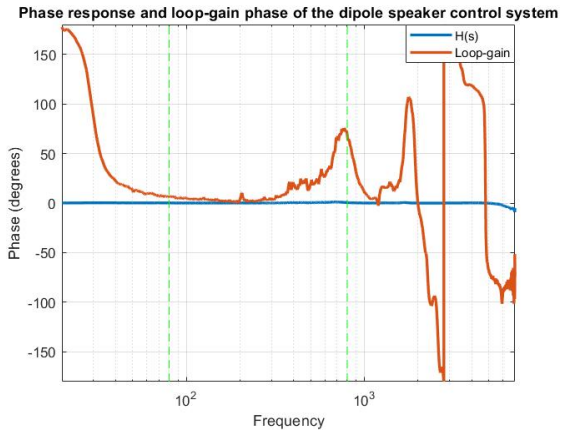

(b) The phase response of the system.

Figure E.1: Initial system response without any signal processing done in the controller.

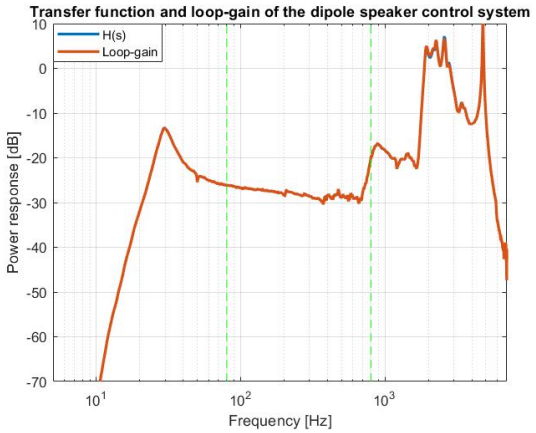

(a) The frequency response of the system.

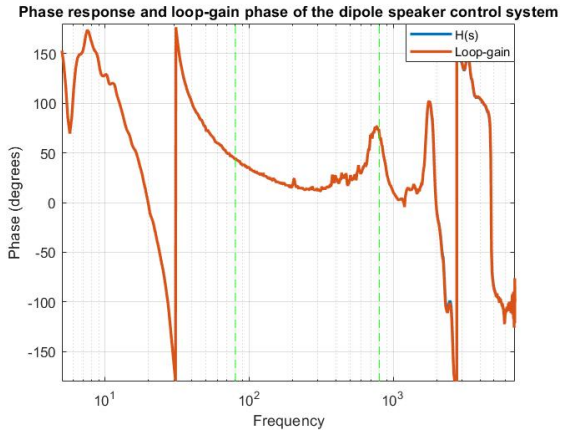

(b) The phase response of the system.

Figure E.2: The system response after adding a simple high-pass filter in the controller.

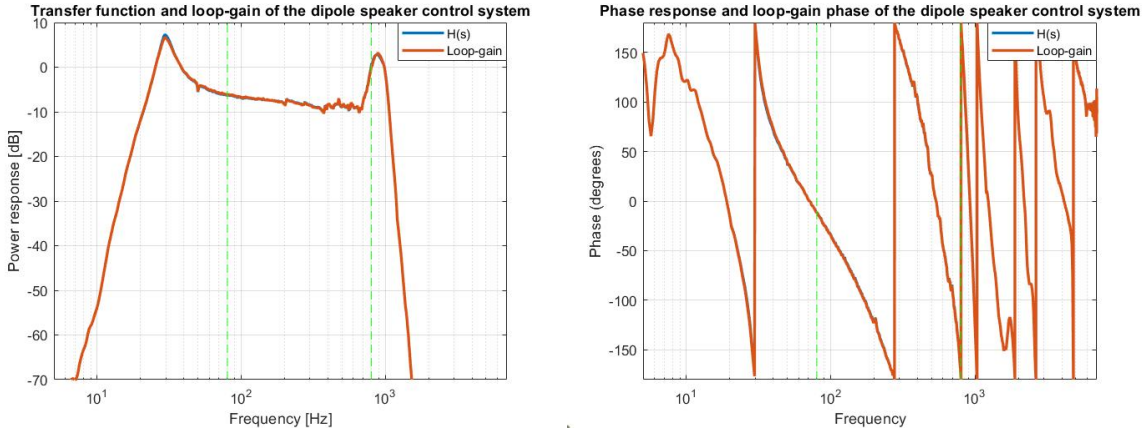

(a) The frequency response of the system.

(b) The phase response of the system.

Figure E.3: The system response after adding a simple high-pass filter and a high order low pass filter in the controller.

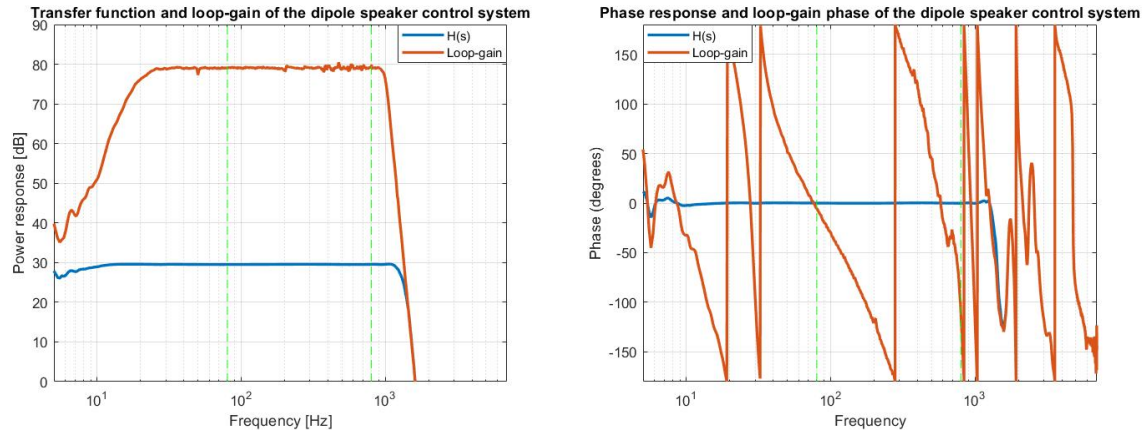

(a) The frequency response of the system.

(b) The phase response of the system.

Figure E.4: The system response after adding extra loop-gain such that stability still holds

F

Total system

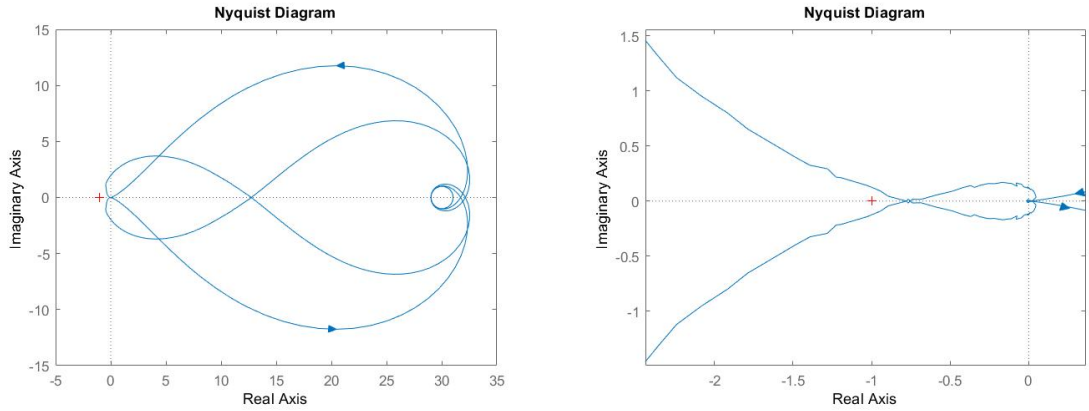

(a) The Nyquist plot before adding additional gain

(b) The Nyquist plot after adding additional gain

Figure F.1: The nyquist plots showing the stability of the system before and after additional loop-gain is added.

Component	Maximum output voltage
Adder	$3.8mV$
Voltage amplifier	$1.14V$
ADAU 1777 chip	$900mV$
Voltage to current amplifier	$27V$
Mono-pole Speaker	$30.2V$
System gain	$1.0067V$

Table F.1: The maximum output voltage found for each component in the dipole speaker control system for an input sinusoid of amplitude $1V$.

G

Noise in the system

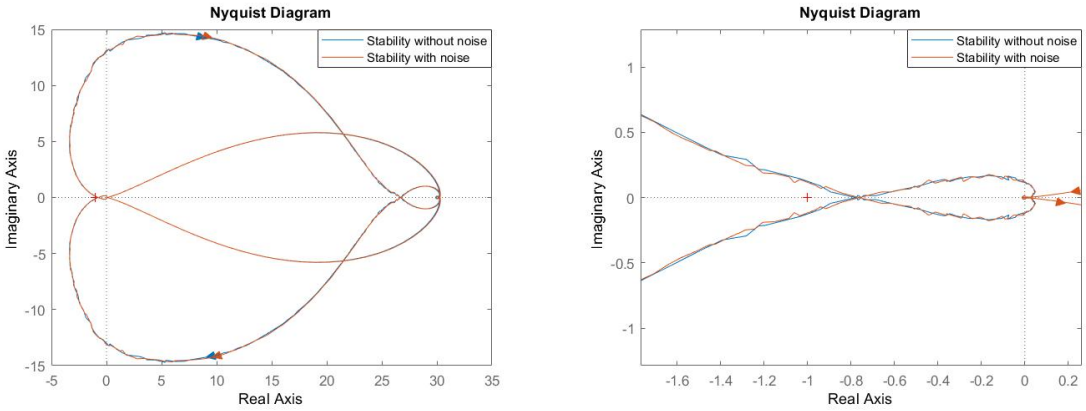

(a) The nyquist plot with and without added noise to the system

(b) The nyquist plot zoomed in to the -1 point

Figure G.1: The nyquist plot of the control system surrounding the dipole speaker with and without added noise sources

Bibliography

[1] D. Vlaardingenbroek A. Avdeev, H. Diahlani. *Voltage to current amplifier.* TU Delft, 2020.

[2] C. Varon A. van der Veen. *Practicum EE2T11 Telecommunication: Signals and Systems.* TU Delft, 2020.

[3] *Four-ADC, Two-DAC, Low Power Codec with Audio Processor, ADAU1772.* Analog Devices, 2014. URL https://www.analog.com/media/en/technical-documentation/data-sheets/ADAU1772.pdf. Rev. 0.

[4] *Four-ADC, Two-DAC, Low Power Codec with Audio Processor, ADAU1777.* Analog Devices, 2016. URL https://www.analog.com/media/en/technical-documentation/data-sheets/ADAU1777.pdf. Rev. 0.

[5] Martin Rune Anderse. Compensation of nonlinearities in transducers. Master's thesis, Technical University of Denmark, 2005. URL http://www2.imm.dtu.dk/pubdb/views/edoc_download.php/3871/pdf/imm3871.pdf.

[6] L.F. Chaparro. *Signals and systems using MATLAB.* Academic Press, 2015. ISBN 978-0-12-394812-0.

[7] D. Chiang. Tuned deconvolution digital filer for elimination of loudspeaker output blurring, 1990. URL https://patentimages.storage.googleapis.com/14/d7/26/27756c6874d0de/US5185805.pdf.

[8] M.J. Demler. *Flash A/D Application.* Academic Press, 1991. ISBN 978-0-122-09048-6.

[9] C.E. Korman F. Mohd-Yasin, D.J. Nagel. Noise in mems, 2009.

[10] A. Emami-Naaeini G.F. Franklin, J.D. Powell. *Feedback Control of Dynamic Systems 7th.* Pearson Education Limited, 2015. ISBN 978-1-292-06890-9.

[11] S.H. de Koning J.A. Klaassen. Bewegingstegenkoppeling bij luidsprekers, 1968.

[12] D. Jarman. A brief introduction to sigma delta conversion, 1995. URL https://ecee.colorado.edu/~mcclurel/intersilan9504.pdf.

[13] W. Klippel. Loudspeaker nonlinearities - causes, parameters, symptoms. *Audio Engineering Society*, 54(10):907–939, 2006. URL https://www.klippel.de/fileadmin/_migrated/content_uploads/Loudspeaker_Nonlinearities\T1\textendashCauses_Parameters_Symptoms_01.pdf.

[14] W. Klippel. Nonlinear losses in electro-acoustical transducers, 4 2012. URL https://hal.archives-ouvertes.fr/hal-00810564/document.

[15] F. A. Levinzon. Fundamental noise limit of piezoelectric accelerometer. *IEEE Sensors Journal*, 4(1):108–111, 2004. URL https://ieeexplore-ieee-org.tudelft.idm.oclc.org/document/1261869.

[16] Tymphany HK LTD, 2017. URL https://www.parts-express.com/peerless-by-tymphany-830669-12-paper-cone-sls-subwoofer--264-1118#lblProductDetails.

[17] A. Montagne. Slicap. https://www.analog-electronics.eu/slicap/slicap.html, 2009-2020.

[18] K. Oyen. Compensation of loudspeaker nonlinearities. Master's thesis, Norwegian University of Science and Technology, 2007.

[19] PirateLogic, 2019. URL https://piratelogic.nl/?p=en.littleone.

[20] P.P.L. Regtien. *Electronic instrumentation.* Delft Academic Press /VSSD, 2015. ISBN 9789065623799.

[21] Grimm Audio R.H. Munnig Schmidt, RMS Acoustics & Mechatronics. Loudspeaker technique white papers, 2017. URL https://www.grimmaudio.com/publications/loudspeaker-technique-white-papers/.

[22] L.W. Couch II. *Digital and Analog Communication Systems*. Pearson, 8 edition, 2013.

[23] R.H. Munnig Schmidt. Motional feedback theory in a nutshell, 2017. URL https://rmsacoustics.nl/papers/whitepaperMFBtheory.pdf.

[24] Spectrum Software. Microcap 12. http://www.spectrum-soft.com/contact.shtm, 1980-2019.

[25] *OPA177 Precision Operational Amplifier*. Texas Instruments, 2000. URL https://www.ti.com/product/OPA177.

[26] M.L. Wilson. Laser sensor capable of measuring distance, velocity and acceleration, 1995.

[27] Ethan Winer. *The Audio Expert*. New York and London: Focal Press, 2013. ISBN 978-0-240-82100-9.

[28] G. T.-C. Chiu Y. Li. Control of loudspeakers using disturbance-observer-type velocity estimation. *IEEE/ASME Transactions on Mechatronics*, 10(1):111–117, 2005. URL https://ieeexplore-ieee-org.tudelft.idm.oclc.org/stamp/stamp.jsp?tp=&arnumber=1395873.